Biosensors and Bioelectronics 184 (2021) 113249

Contents lists available at ScienceDirect

Biosensors and Bioelectronics

journal homepage: http://www.elsevier.com/locate/bios

Integrated non-invasive biochemical and biophysical sensing systems for health and performance monitoring: A systems perspective

By Murat A. Yokus [a], Michael A. Daniele [a,b,*]

[a] Department of Electrical & Computer Engineering, North Carolina State University, 890 Oval Dr., Raleigh, NC, 27695, USA
[b] Joint Department of Biomedical Engineering, North Carolina State University and University of North Carolina at Chapel Hill, 911 Oval Dr., Raleigh, NC, 27695, USA

ARTICLE INFO

Keywords:
Wearable
Biosensor
Sweat
Epidermal
Multiplexed systems

ABSTRACT

Advances in materials, bio-recognition elements, transducers, and microfabrication techniques, as well as progress in electronics, signal processing, and wireless communication have generated a new class of skin-interfaced wearable health monitoring systems for applications in personalized medicine and digital health. In comparison to conventional medical devices, these wearable systems are at the cusp of initiating a new era of longitudinal and noninvasive sensing for the prevention, detection, diagnosis, and treatment of diseases at the molecular level. Herein, we provide a review of recent developments in wearable biochemical and biophysical systems. We survey the sweat sampling and collection methods for biochemical systems, followed by an assessment of biochemical and biophysical sensors deployed in current wearable systems with an emphasis on their hardware specifications. Specifically, we address how sweat collection and sample handling platforms may be a rate limiting technology to realizing the clinical translation of wearable health monitoring systems; moreover, we highlight the importance of achieving both longitudinal sensing and assessment of intrapersonal variation in sweat-blood correlations to have the greatest clinical impact. Lastly, we assess a snapshot of integrated wireless wearable systems with multimodal sensing capabilities, and we conclude with our perspective on the state-of-the-art and the required developments to achieve the next-generation of integrated wearable health and performance monitoring systems.

1. Introduction

The history of diagnostics dates back to ancient Egypt and Mesopotamia, where the earliest physicians made diagnoses and treatment using their senses (Berger 1999). In medieval times, physicians used palpation to understand diseases related to the heart and lungs, and utilized coloration of the skin, smelling, and tasting of wounds, breath, sweat, and urine to describe dysfunctions related to the digestive tract, liver, and spleen. With the invention of the stethoscope, microscope, endoscope, thermometer, X-rays, electrocardiogram, and other medical devices, significant advancements were made in the study of histology, cytology, and human physiology. The medical diagnostics progressively moved from qualitative and subjective examinations by the physicians to new sensing systems, in which the data could be recorded, analyzed, and compared with the data recorded in the past. With the advent of telemetry, it became common to monitor the physiological condition of patients at a distance from the clinic. The remote home-based monitoring enabled the exchange of discrete medical data (blood pressure cuff, glucose meters, pulse oximeters, or heart monitors) between a patient at home and medical personal at clinics using phone or wireless technology.

Wearable health monitoring systems provide the opportunity to monitor users passively or on-demand while the users engage in usual daily activities. These wireless systems usually necessitate body-worn systems and are applicable for specific medical conditions where the home-based telemonitoring is not adequate. Some of the best examples of wearable systems are ECG Holter monitor and continuous glucose monitors (CGMs) (Galli et al., 2016; Hovorka 2006). Often abnormal heart conditions and unforeseen changes in blood glucose levels may not be present on routine clinical visits. Ambulatory monitoring with these systems can detect periodic arrhythmias, monitor large fluctuations in blood glucose levels, and provide clinicians with a snapshot of the health condition of patients. Another use of mobile wearable systems is in on-demand and post-intervention monitoring, where the recovery of an athlete or patient from an injury or a medical condition (*e.g.*, heart attack or peripheral artery disease) can be monitored continuously, and

* Corresponding author. Department of Electrical & Computer Engineering, North Carolina State University, 890 Oval Dr., Raleigh, NC, 27695. USA.
E-mail address: mdaniel6@ncsu.edu (M.A. Daniele).

https://doi.org/10.1016/j.bios.2021.113249
Received 26 January 2021; Received in revised form 9 April 2021; Accepted 12 April 2021
Available online 19 April 2021

efficacy of treatments and planning of subsequent medication can be assessed (Haveman et al., 2019). The usage of the ambulatory monitoring can be extended to emergency monitoring of first responders, fire fighters, and aircraft pilots, and the performance parameters can be remotely monitored by qualified staff with the aim of survival management (Lorincz et al., 2004; Michahelles et al., 2003).

The architecture of a wearable health monitoring system consists of external sensors, a central processing unit, analog-to-digital converter (ADC), a wireless interface, battery, and energy management unit (Fig. 1). The external sensors for mobile applications can include sensors for monitoring heart and lung activity (ECG, respiration, oxygen saturation, and heart rate), biochemical composition (pH, glucose, hormones, and proteins), and body characteristics (temperature and activity). These sensors convert electrical, mechanical, chemical, and radiant energy into an electrical signal that can be recorded by the processing unit. Each biosensor may require specific pre-processing and amplification stages depending on the output type of the sensors (*e.g.*, voltage, current output), dynamic range, and frequency of the biosignals. While typical pre-processing stages are low-noise amplifiers and anti-aliasing filters, additional components may be added depending on the sensor type, such as potentiostats for biochemical sensors and light-emitting diodes, photodetectors, and current drivers for optical sensors. Filtering is performed to reduce the contribution of high-spectral components as well as to remove the external noises, such as motion artifacts, which is followed by an ADC stage with adequate resolution to acquire biosignals. The processing unit and data storage modules acquire, process (feature extraction and classification), store, and transmit the physiological data. The wireless interface includes wireless communication technologies, such as mid-range RF communications (Bluetooth and Zigbee) and short-range inductively coupled links (RFID and NFC), for the transfer of the physiological data to a nearby device or computer (Yuce 2010). The connection of these devices with medical servers over the internet is carried out via GSM/CDMA/LTE/5G cellular networks or Wi-Fi, where physicians and caregivers are connected through a network of health servers and databases. Battery and energy management unit powers the rest of the system and regulates the voltage required for the parts of the system. The design and relevance of the wearable systems usually determine their final use, and in most cases, will be contingent on the requirements of mobile monitoring applications, such as critical importance of physiological biomarker and frequency of device usage.

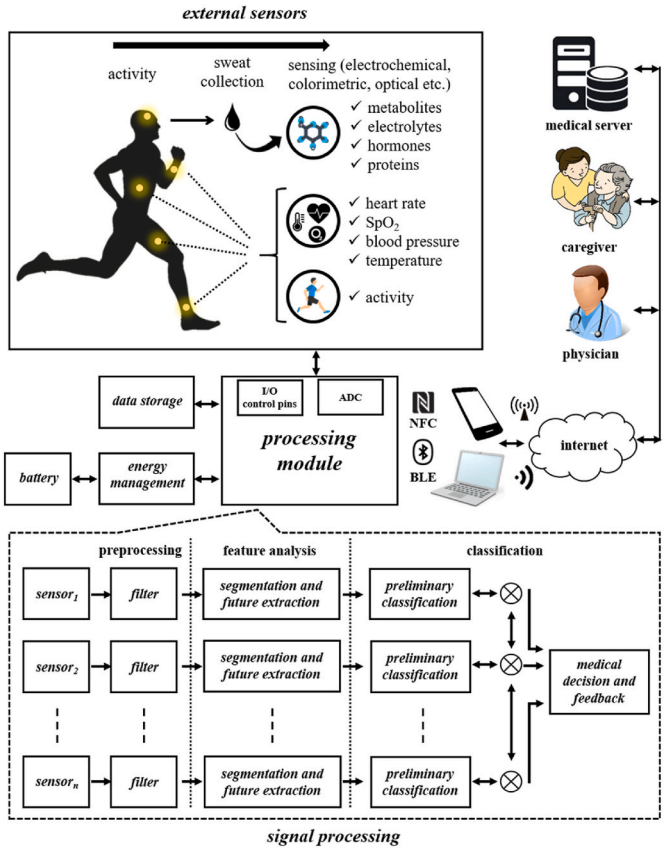

Fig. 1. A schematic illustration of the architecture of wearable multimodal health monitoring systems. The system consists of external sensors, a central processing unit, analog-to-digital converter (ADC), a wireless interface, battery, and energy management unit. The processing module acquires, processes, and transmits the signals from external biochemical and biophysical sensors. The wearable systems have the capability of sampling and analyzing biofluid of interest (*e.g.,* sweat) via biochemical sensors and can wirelessly send the biochemical information with other physical, sensory data to a smartphone or a tablet. The medical data from these devices is sent to the medical servers (*i.e.*, cloud) via cellular networks or Wi-Fi, where physicians and caregivers are connected through a network of health servers and databases to provide feedback, treatment, prognosis, and diagnosis based on the history of the clinically relevant data.

The integration of wearable health monitoring systems with the body can have different configurations based on the application, source of biosignals, portability, ease of use, and user comfort (Guk et al., 2019). Commercial wearable devices, such as wristwatches, armbands, chest patches, and smart clothing, have been developed by various companies to monitor blood pressure (iHealth), activity and sleep (iHealth, Fitbit, Apple, and Garmin), pulse oximeter (iHealth and Nonin Medical), cardiovascular health (Hexoskin, Zephyr strap, MC10 BioStamp), and glucose (GlucoWatch G2 Biographer and GlucoTrack) (Apple 2020; Fitbit 2020; GlucoTrack 2020; Hexoskin 2020; iHealth 2020a, b; Nonin Medical 2020; Samsung 2020; Vashist 2012; Zephyr 2020). The employment of these systems can range from fitness/wellness monitoring and disease prognosis to anomaly detection and medical diagnosis. Despite the popularity of wearables, user acceptance is limited to specific areas, mostly due to their limited sensing capabilities. This condition restrains their widespread use in health and clinical applications as most of the clinical conditions cause changes in body biochemistry. As such, wearable systems with multimodal sensing capabilities (physical and biochemical) can provide a wealth of information for a broader understanding of health conditions and disease states.

The new class of skin-worn wearable systems can collect and sense biological fluids, such as sweat, in addition to sensing other physiological parameters. Detection of analytes from eccrine sweat glands offers some advantages over other biofluids (*e.g.,* blood, tear, and urine) due to its ease of sampling, non-invasiveness, and availability of the eccrine sweat glands across the body. Sweat, specifically, contains electrolytes, metabolites, proteins, and hormones, and may offer real-time molecular analysis of the physiological state (Baker 2019; Kumar et al., 2016; Robinson and Robinson 1954). The ability to accommodate physical and biochemical sensors on a single wearable platform with on-board processing and wireless connectivity enables new classes of biochemical sensors that can address the needs of clinicians, patients, athletes, and daily users (Fig. 1).

The design of such wireless, skin-worn systems should meet numerous specifications at the sensor, device, and system-levels. The sensor-level requirements include stability (pH, temperature, ionic strength, and humidity), sensitivity, and limit of detection of a sensor for the detection of a biochemical analyte or a physical parameter (Bandodkar et al., 2016). The device-level requirements embody the design of microfluidics for sweat extraction and collection to minimize analyte degradation, sweat evaporation, and contamination from the skin (Heikenfeld 2016). In addition to the fluid handling, ease of wear, non-invasiveness, no toxicity, and unobtrusiveness are essential for wearable devices for the mitigation of skin-device mechanical mismatch, skin irritation, and motion artifacts (Gemperle et al., 1998). The system-level requirements comprise real-time data acquisition,

power consumption and battery lifetime, communication and mesh network coverage, fault tolerance (robustness to the common interferences), decision support and user interface, multisensory data management and data mining, data encryption and security, standardization, cost, and scalability (Kulkarni and Öztürk 2007; Pantelopoulos and Bourbakis 2008). All the design requirements make the design of skin-worn wearable systems a tedious process to meet the needs of the intended application, such as the selection of optimal sensors, multi-level integration and fabrication, and electronic system design.

This review highlights the research and development in skin-worn, sweat-based wearable sensors, integration with biophysical and biophotonic sensors, and systems thereof, as reported in the last five years for applications towards health and performance monitoring. It is aimed to be complementary to the existing reviews in this field (Bandodkar et al. 2016, 2019c; Bariya et al., 2018a; Heikenfeld et al., 2017; Kim et al., 2019; Legner et al., 2019; Ray et al., 2019; Sempionatto et al., 2020a; Takei et al., 2019) by summarizing the current research on biochemical (metabolites, electrolytes, oxygen, and other chemicals) and biophysical (sweat rate and temperature) sensors and featuring examples of wearable multimodal systems with a focus on their system-level operation. With that in mind, Sections 2-4 summarize sweat sampling and collection techniques as well as biochemical and biophysical sensors in current wearable devices. Subsequently, the platforms which demonstrate multimodal biochemical and biochemical sensing capabilities are evaluated. We ultimately discuss and present related challenges and our perspectives on wearable systems in the context of prolonged physiological monitoring.

2. Wearable biochemical sensors

2.1. Sweat extraction and sampling methods in wearable sensors

The extraction and collection of sweat is vital for accurate and reliable detection of analytes in real-time sweat sensing applications because sweat generation varies between individuals and even exhibits intrapersonal regional variation (Patterson et al., 2000; Sato and Sato 1983). As such, the correlation of sweat constituents to relevant physiological predictors has been difficult to define. There are few reports of the clinical utility for measuring metabolites, *e.g.,* glucose and lactate, and electrolytes, *e.g.,* Na^+ and K^+, because sample volumes, secretion rates, filtration, active analyte channels, variable pH and salinity, analyte breakdown and other confounding factors are present (Heikenfeld et al., 2019; Nyein et al., 2019).

Accordingly, technologies for the controlled stimulation, accurate collection of sweat, and measurement of sweat rate must be integrated in any wearable health monitoring system. Extraction of sweat from skin can be accomplished by thermal bathing, exercise, or local iontophoretic stimulation. Once an adequate amount of sweat is accumulated on the skin surface, it needs to be further sampled and stored to prevent sweat loss and any potential degradation of analytes. Traditional sweat sampling techniques involve whole body-washdown technique and sweat collection with absorbent patches and Macroduct® (Liu et al., 2020). The whole body-washdown technique is the gold standard for the measurement of total sweat loss and its composition (Baker et al., 2009). In this method, subjects exercise on a cycle ergometer in a sealed plastic box. Upon completion of the exercise, subjects, the plastic box, clothes, and equipment are rinsed with deionized water to collect sweat for further analysis. This method involves complex steps and controlled lab settings; therefore, it does not apply to field settings. The absorbent patches are usually applied at specific locations on the body, such as the forearm, upper arm, thigh, and lumbar area, along with a supporting outer membrane (Baker et al., 2016; Kintz et al., 1996). The collected sweat is weighed for sweat loss or extracted and analyzed for further analysis. Although this method is simple, its results vary with different sweat regions, and it may overestimate the analyte concentration as compared to the body-washdown technique. The absorbent patches may also block the sweat ducks (hydromeiosis effect) and affect the sweat rate if the sweat pool is formed on the skin surface. Macroduct®, a sweat collecting device for sweat rate and composition analysis, allows collection of sweat in its spiral plastic tubes and minimizes hydromeiosis (Matzeu et al., 2016). The Macroduct® limits total sweat volume to approximately 85 μL and does not include any integrated sweat-rate measurement. With that said, the Macroduct® can be serially imaged, and sweat volume per unit time can be calculated (Brueck et al., 2018; Matzeu et al., 2016). The traditional sampling methods require trained personnel, complex procedures, and may suffer from low sweat volumes. They are susceptible to sample evaporation, regional and varying sweating rates, potential sample degradation between collection and analysis steps, making it not suitable for real-time and dynamic sweat monitoring. Therefore, novel approaches and miniaturized sampling devices have been proposed to mitigate some of the challenges of the traditional methods that enable in-situ sweat collection and analysis on a single sensing device.

Engineering the skin-sensor interface to minimize the contamination from the skin is one of the essential design considerations in sweat sampling. The gap between skin surface and sensor determines the volume of the sampled sweat as well as the time required to thoroughly flush out the old sweat from the skin-sensor interface (Sonner et al., 2015). Uneven skin surface, presence of hair, and low sweat rates from the sweat glands increase the time required for replenishment of old sweat; consequently, it increases the potential of skin contamination from cosmetics or bacteria. Heikenfeld's group proposed a new oil-membrane approach to reduce the sensing sample volumes from μL to nL to minimize the analyte contamination (Peng et al., 2016). A micro-porous polycarbonate membrane is coated with a water-soluble polyvinyl alcohol (PVA) polymer and a cosmetic-grade oil and placed onto the skin (Fig. 2a). Isolating the sweat only to the region above the sweat ducts reduces sweat sampling time to the order of several minutes, and it blocks the low oil solubility contaminants from the skin surface. This method may make the wearable sensor susceptible to biofouling from the lipophilic analytes and the dissolved PVA membrane.

An alternative way of engineering the skin-sensor interface is the placement of sweat-absorbing materials at the skin-sensor interface. The absorbent materials are not only used for absorbing sweat but also for eliminating the direct skin contact, skin irritation, and reducing the motion artifacts in wearable systems. Fig. 2b shows a sponge-like substrate for the collection and analysis of sweat (Huang et al., 2014). Its integration with thin and stretchable electronics enabled assessment of sweat volume via a dielectric change and colorimetric analysis of sweat composition, such as pH, copper, and iron concentration. When the pores of the absorbent material were filled with sweat, it caused changes in color and dielectric properties of the absorbent material, which then could be interrogated with a digital camera and near field communication device nearby. Although colorimetric sensing with the absorbent material looks promising, on the system level, the radio frequency characteristics of the sensing device are sensitive to mechanical stretching, salinity, and ionic content of sweat.

Directing sweat from the skin surface toward a sensing area is one of the unconventional approaches for analyte sensing. This method is usually achieved either by confining the available sweat on the skin surface to the well-defined sensing sites or transporting it away from the skin surface to the sensor for chemical analysis. Fig. 2c demonstrates a flexible platform with hydrophobic and hydrophilic regions for multiplexed analyte sensing of pH, chloride, glucose, and calcium (Wang et al., 2017). The hydrophobic areas were achieved by the roll-to-roll coating of nanodendritic silica, which was followed by oxygen plasma to define hydrophilic sensing microwells. The hydrophobic regions limited wetting only to the hydrophilic microwells and enabled colorimetric detection of analytes in the indicator embedded microwells via a nearby camera. This approach offers a facile semi-quantification of sweat, but it fails to achieve real-time monitoring of sweat. Wang et al. designed a sweat collection channel mounted on the forehead for the

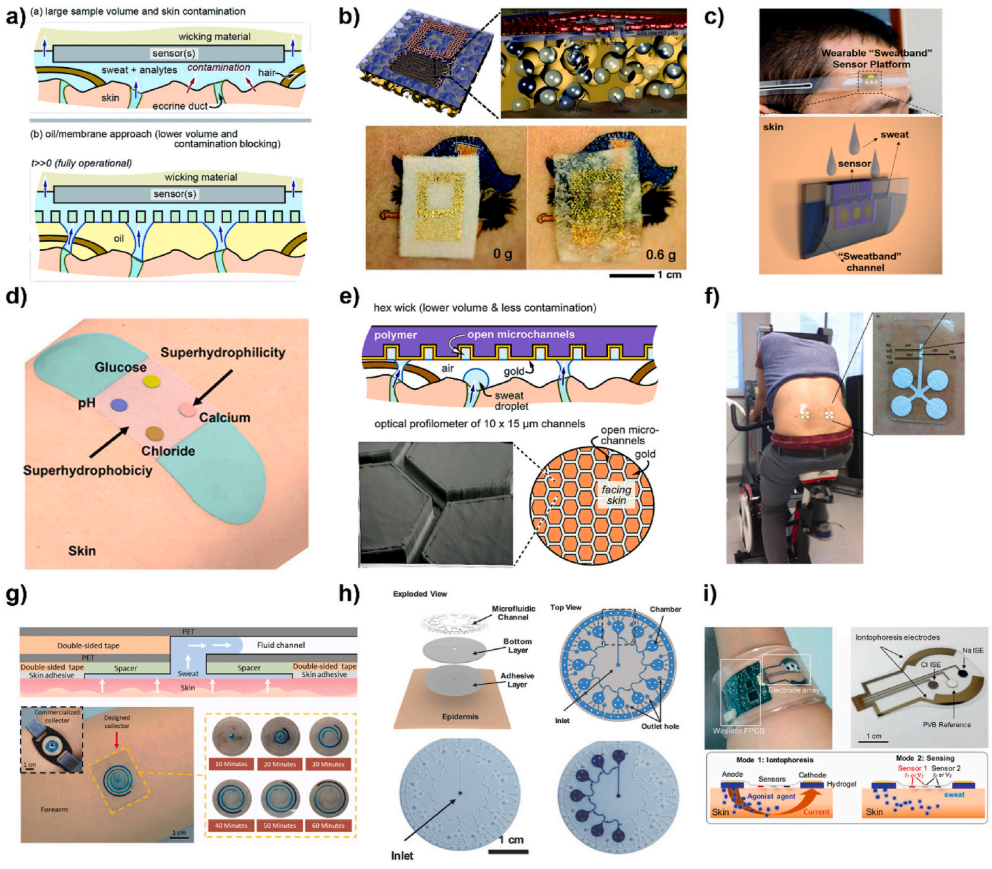

Fig. 2. Sweat extraction and sampling methods in wearable systems. **a)** An oil-membrane approach for sweat sampling. Reproduced with permission (Peng et al., 2016). Copyright 2016, The Royal Society Chemistry. **b)** An absorbent porous substrate for sweat collection. Reproduced with permission (Huang et al., 2014). Copyright 2014, WILEY-VCH Verlag GmbH & Co. **c)** A silicone headband for guiding sweat to the sensing device. Reproduced with permission (Wang et al., 2017). Copyright 2017, American Chemical Society. **d)** Superwettable flexible band for sweat sampling. Reproduced with permission (He et al., 2019). Copyright 2019, American Chemical Society. **e)** A hexagonal network for transport and sampling of low sweat volumes. Reproduced with permission (Twine et al., 2018). Copyright 2018, The Royal Society Chemistry. **f)** A paper microfluidic channel for sweat transport and evaporation. Reproduced with permission (Anastasova et al., 2017). Copyright 2017, Elsevier. **g)** 3D microfluidic channels for sweat sampling and measurement of sweat loss. Reproduced with permission (Lin et al., 2019). Copyright 2019, The Royal Society Chemistry. **h)** A microfluidic patch with capillary bursting valves for chrono-sampling of sweat. Reproduced with permission (Choi et al., 2017a). Copyright 2017, WILEY-VCH Verlag GmbH & Co. **i)** A fully integrated platform for iontophoretic sweat stimulation and sensing. Reproduced with permission (Emaminejad et al., 2017). Copyright 2017, National Academy of Sciences USA.

collection of sweat (Fig. 2d) (He et al., 2019). The exercise-induced sweat was transported to the sensor surface and enabled real-time measurement of sodium levels with the wearable system.

With the advancement in materials and fabrication techniques, skin-like and miniaturized microfluidic devices have been developed and integrated with wearable systems for the passive collection of sweat and sensing of analytes (Bandodkar et al. 2019a, 2019c; Koh et al., 2016). These epidermal microfluidic devices take advantage of the secretion pressure of sweat glands and capillary pressure of microfluidic channels to guide sweat from the skin surface to the sensing sites (Choi et al., 2017b). Design of channel size, microfluidic chamber volume, and shapes are required to achieve operation across the range of sweat rates. Typical sweat rates monitored from human subject testing was 3–5 μL min^{-1}, but the devices could accommodate up to 10 μL min^{-1} which encompasses most physiologically-relevant sweat rates. These novel devices are designed to achieve efficient spatiotemporal sampling of sweat, reduced sweat evaporation, and minimal contamination from the skin surface; however, they rely on the active excretion of sweat due to thermal or exercise stimulation.

Heikenfeld et al. designed a hexagonal network of gold-coated microchannel for rapid transport of low sweat volumes (<100 nL) to the sensing electrodes (Fig. 2e) (Twine et al., 2018). The gold surface was modified with peptides to have a biocompatible and hydrophilic surface. Engineering the design and surface of the wicking surface endowed the device with increased fluid transport and minimal analyte loss. However, the fluid coupling between the hexagonal network and sensing electrode was made with rayon, which may cause analyte depletion as well as erroneous readings due to insufficient electrode contact in real-time monitoring. In another study, Anastasova et al. used a paper microfluidic channel to avoid the problems associated with sweat accumulation on the skin surface (Anastasova et al., 2017). As sweat entered the channel, it was drawn across the length of the paper channel via capillary forces (Fig. 2f). The transported sweat was collected at the end of the channel (reservoirs), where it was continuously evaporated. The fluid sampling, transport, and evaporation enabled the real-time measurement of pH, sodium, and lactate in sweat with a wireless system. While the use of paper microfluidics is beneficial for biofluid storage and *post facto* analysis, trapping the biofluid in the matrix limits options for accurately monitoring sweat rate and sweat volume collected. Anastasova et al. do not report either. Lin et al. devised a simple and inexpensive fabrication method for biofluid sampling, manipulation, and sensing (Lin et al., 2019). The method involved laser cutting and vertical alignment of flexible film sheets and double-sided tapes to form 3D and complex microfluidic architectures, such as devices for sweat collection, sample filtration, and biofluids actuation and sensing (Fig. 2g). The high throughput manufacturing technique presented an alternative, low-cost disposable solution to minimize challenges related to contamination from old sweat residues and sensor biofouling. In another study, Choi et al. designed a skin conformable microfluidic patch for chrono-sampling of lactate, sodium, and potassium (Choi et al., 2017a). The device consisted of a network of microfluidic channels that incorporates capillary bursting valves that allow the fluid passage at different fluid pressures, enabling sequential filling of multiple microreservoirs (Fig. 2h). The microfluidic devices captured and stored sweat volumes up to 6 μL, depending on microfluidic design, and allowed extraction of the collected fluids for *ex situ* analysis. Despite its remaining challenges related to low sweat collection volumes and undesired adsorption of some analytes (*i.e.*, hormones and vitamins) on the microfluidic walls, this proposed microfluidic patch enables temporal measurement of some of the physiologically abundant biomarkers in sweat. These sweat collection methods require prolonged active exercise for the activation of sweat glands and sweat generation,

making it inconvenient for elderly and sedentary subjects.

To achieve on-demand or passive sweat collection and monitoring of analytes with wearable sweat extraction and sensing platforms are needed for in situ sweat analysis. Emaminejad et al. developed a wireless system with an electronic iontophoresis interface and sensing electrodes for real-time chloride, sodium, and glucose monitoring (Emaminejad et al., 2017). The iontophoretic stimulation was carried out with a pair of sweat induction electrodes that interfaced the skin with a sweat gland secretory stimulating agonists, such as acetylcholine or pilocarpine (Fig. 2i). The induced sweat was sensed using sensing electrodes covered with a water-absorbent rayon pad to maintain a reliable sensor reading. Long-term iontophoretic sweat generation may have the potential of electrode corrosion, resulting in significant sensor drift or degradation of functional sensing chemistry. In addition, local skin irritation can be realized by prolonged stimulation and delivery of secretory stimulating agonists. Carbachol has been reported as an alternative agonists to achieve extended stimulation for greater than 24 h and at a lower iontophoretic current (Hauke et al., 2018a; Simmers et al., 2018).

Analogous to iontophoretic stimulation of sweat, a novel chemically-induced method for sweat extraction and sampling was reported by Velev et al., in which chemical potential is exploited to drive sweat from the skin to a collection device. Tuning the osmotic pressure across the skin-device interface is used to drive fluid from the skin into a hydrogel containing high-osmolar glucose or glycerol (Saha et al., 2021; Shay et al., 2020). These sweat collection devices are unique in being zero-power, which may enable more clinically-relevant extraction over days. Such devices exhibited *in vitro* extraction from hrs to multiple days, and *on-body* extraction was tested for up to 2 h; the latter being potentially limited by the fundamental biology of the sweat production process.

To date, sweat sampling methods included novel approaches for engineering the device-skin interface, iontophoresis, exploiting chemical potential gradients, and transporting the sweat away from the skin with a paper or polymeric microchannels. A summary of representative sweat collection methods, sample volumes, and sampling time is presented in Table 1. All reported techniques aim to consistently sample sweat with reduced skin contamination, minimal sweat evaporation, and prolonged or on-demand sensing, and delivery of sweat to the sensing sites via these methods enables the detection of analytes via colorimetric, fluorometric, or electrochemical methods (Choi et al., 2019; Sekine et al., 2018; Zhang et al., 2019b). Yet, few reports have fundamentally defined how the stimulation and collection rates affect the sweat constituency; moreover, while many devices can collect microliters of sample during active or induced sweating, very few reported systems are operated under passive conditions, *i.e.,* at resting sweat rates (from pL to $nL \cdot min^{-1} \cdot cm^{-2}$) and volumes (<100 nL). Further investigation and response analysis of novel devices like “osmotic pumps”, alternative iontophoretic agonists, and nanofluidics may elucidate better means to collect sweat in resting users, control sampling rates, assess dilution effects, and define sweat-blood correlation.

Table 1
Representative specifications for sweat collection devices.

Wearable Technique	Sweat Sample Volume	Collection Method	Collection Time	References
Paper Microfluidics	<15 μL	Exercise	–	Anastasova et al. (2017)
	~40 μL	Exercise	30 min	Parrilla et al. (2019a)
	–	Exercise	30 min	Li et al. (2021)
Microfabricated Films & Membranes	<1 nL	*Passive*	–	Peng et al. (2016)
	20 nL	–	–	Garcia-Cordero et al. (2018b)
	150 nL	–	–	Garcia-Cordero et al. (2018a)
	<150 nl cm^{-2}	Chemical Agonist + Iontophoresis	<3 min	Twine et al. (2018)
Direct Skin-Sensor Contact	*	Chemical Agonist + Iontophoresis	–	Emaminejad et al. (2017)
	*	Exercise	–	Gao et al. (2016a)
Epidermal Microfluidics	–	Exercise	–	Kim et al. (2018b)
	58 μL	Exercise	<6 h	Bandodkar et al. (2019b)
	14 μL	Exercise	<50 min	Nyein et al. (2018a)
	1–15 μL	Hot Shower	<16 min	Zhang et al. (2019b)
	27–73 μL	Exercise; Sauna	~20 min	Choi et al. (2017a)
Absorbent Polymers & Gels	~1.8–4 μL	Exercise; *Passive*	1 h; 2 h	Saha et al. (2021) Shay et al. (2020)
	200–400 μL	Exercise	2 h	Huang et al. (2014)
	1–16 μL	Exercise	–	Lee et al. (2017a)
	0.4–2 μL	Exercise	–	He et al. (2019)
	<1 μL	*Passive*	5 min	Lin et al. (2020)
Macroduct®	50–60 μL	Chemical Agonist + Iontophoresis	30–45 min	**

*Sweat samples are not collected or stored.
*Commercial Specification.

2.2. Biochemical sensing in current wearable devices

2.2.1. Metabolites

Metabolites are small molecules produced in biochemical pathways of human metabolism and involved in a myriad of functions, from energy production to signaling. Metabolites in sweat, such as glucose, lactate, urea, and ethanol, are potential candidates for noninvasive monitoring of human physiology. Glucose, for instance, is the primary source of energy production of the human body and associated with diabetes, Alzheimer’s disease, cognitive impairment, and renal complications (Mergenthaler et al., 2013). Lactate is a primary biomarker of anaerobic metabolism and clinically associated with lactic acidosis. It is the indicator of poor tissue oxygenation (myocardial infarction, sepsis, and hypovolemia), common diseases (diabetes, liver and renal disease, and leukemia), and drugs and toxins (Kreisberg 1984).

Both glucose and lactate are regarded as a critical health indicators and have received significant attention for the development of noninvasive wearable systems, but before assessing the array of wearable systems for metabolite analyses, it is important to note that the clinical value of analyzing sweat constituency is still being defined. While systemic and regional concentrations of metabolites have been broadly deployed in clinical diagnostics, *i.e.,* basal metabolic and protein-metabolite panels, the value of monitoring metabolite concentrations in sweat, as correlates of acute or chronic conditions, is still under investigation. A recent evaluation by Javey et al. concluded that significant variation in concentrations of basic sweat constituents (Na+, K+, and glucose) is realized at different locations on the body; moreover, simple correlations between systemic and iontophoretic sweat glucose concentrations were not strong (Nyein et al., 2019). A recent review by Heikenfeld et al. attribute the significant challenge to determining sweat-blood correlations and define the appropriate clinical value of monitoring sweat metabolites is the limited understanding of the fundamental biology of sweating. They highlight that the underlying biology, including stimulation pathways, secretion rates, filtration, analyte channels, and equilibrium partitioning, must be better understood to use sweat sensor data to make a clinical impact (Heikenfeld et al., 2019). Of these studies and reviews on sweat sensing, the critique of

equilibrium partitioning may prove particularly impactful, as a generalized strategy for predicting sweat-blood correlation is proposed. Specifically, hydrophilic sweat analytes poorly correlate, while lipophilic sweat analytes strongly correlate. This has panned out in the recent literature, as sweat ethanol, a small, exogenous molecule exhibiting both hydrophilic and hydrophobic properties, is reported as having good sweat-blood correlation (Hauke et al., 2018a; Selvam et al., 2016); whereas other claims of sweat-blood correlations for small, hydrophilic molecules (*e.g.,* glucose and lactate) are limited. Lipophilic molecules have shown better sweat-blood correlation, including cortisol and caffeine (Sekar et al., 2019; Tai et al., 2018). With these assessments in mind, we may consider the following presentation of different sweat sensing systems, as starting points to be further integrated with more accurate understanding of sweating, sweat composition, and then correlating measurements to physiological conditions.

The earliest sensors to start assessing metabolite concentrations in sweat with on-body devices were reported by Wang et al. Real-time monitoring of glucose and lactate was accomplished by integrating electrochemical sensing elements in wearable devices (Wang 2008). Jia et al. demonstrated one of the first examples of noninvasive and epidermal lactate sensors (Jia et al., 2013). The lactate sensor was realized by casting a mixture of carbon nanotube (CNT), tetrathiafulvalene, and chitosan on screen-printed carbon electrode. The generation of electric current was based on enzymatic reactions of lactate oxidase (LO_x) with lactate in sweat (Fig. 3a) (Rathee et al., 2016). The tattoo-like electrochemical sensor conformed to the skin surface and was robust against repeated bending and stretching cycles. In another study, a tattoo-based electrochemical sensor with reverse iontophoretic biofluid extraction was demonstrated (Bandodkar et al., 2015). The Prussian blue (PB) printed epidermal sensor was modified with glucose oxidase (GO_x) and chitosan for enzymatic sensing of glucose. A constant current was applied between a pair of electrodes for the extraction of interstitial fluid, and glucose sensing was performed on the cathodic electrode (Fig. 3b). The developed platform is an alternative to invasive and minimally invasive sensing techniques and holds a potential for longitudinal diabetes management. Similarly, a Prussian blue-based glucose or lactate sensor with a microfluidic reservoir was developed by the same research group to minimize direct skin contact and sample evaporation (Martin et al., 2017). The microfluidic channels provided short sampling times and efficient transport of glucose or lactate on the sensing electrodes, where the generated current was detected and then wirelessly transmitted to a computer by a wearable system (Fig. 3c). Imani et al. and Sempionotto et al. integrated lactate sensors with electrocardiogram and potassium sensors, respectively (Imani et al., 2016a; Sempionatto et al., 2017). Fig. 3d shows an epidermal patch with a printed three-electrode electrochemical sensor and two ECG electrodes for wireless lactate and electrocardiogram monitoring. The sensing electrode of the lactate sensor was functionalized with PB mediator and LO_x enzyme. It was separated from Ag/AgCl electrocardiogram electrodes via a printed hydrophobic layer to minimize the electrical crosstalk in the presence of perspiration. During a high-intensity workout, the epidermal patch simultaneously measured the sweat

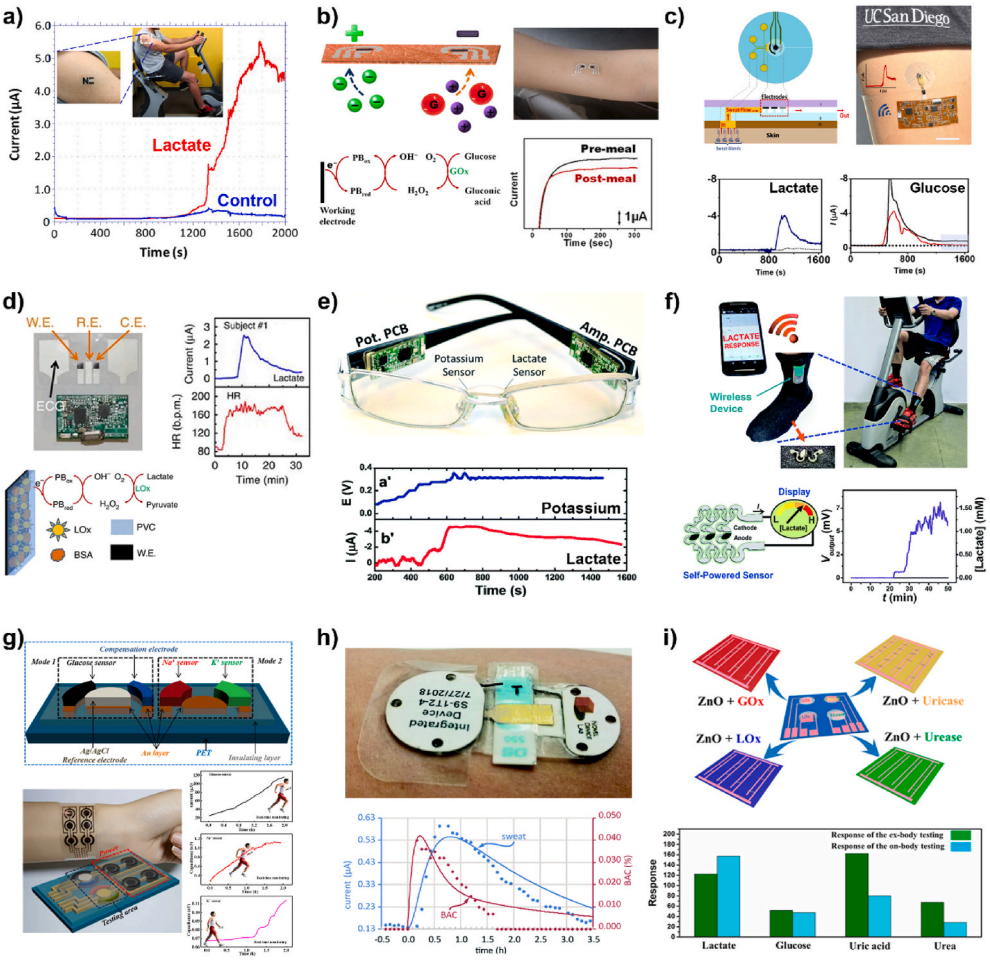

Fig. 3. Examples of electrochemical wearable metabolite sensors. **a)** A printed electrochemical temporary tattoo sensor for lactate sensing. Reproduced with permission (Jia et al., 2013). Copyright 2013, American Chemical Society. **b)** A printed tattoo sensor with reverse iontophoresis option for glucose sensing. Reproduced with permission (Bandodkar et al., 2015). Copyright 2015, American Chemical Society. **c)** An epidermal microfluidic platform with sweat collection and glucose or lactate sensing capabilities. Reproduced with permission (Martin et al., 2017). Copyright 2017, American Chemical Society. **d)** An epidermal sensor for lactate and electrocardiogram sensing. Reproduced with permission (Imani et al., 2016a). Copyright 2016, Creative Commons Attribution 4.0 International License. **e)** Eyeglasses with integrated electrochemical lactate and potassium sensors. Reproduced with permission (Sempionatto et al., 2017). Copyright 2017, The Royal Society of Chemistry. **f)** Self-powered lactate sensing with biofuel cells. Reproduced with permission (Jeerapan et al., 2016). Copyright 2016, The Royal Society of Chemistry. **g)** A self-powered and glucose, Na^+, and K^+ sensing system based on $NiCo_2O_4$ micro-supercapacitors. Reproduced with permission (Lu et al., 2019). Copyright 2019, Elsevier. **h)** A sweat biosensing device with integrated sweat stimulation for ethanol sensing. Reproduced with permission (Hauke et al., 2018b). Copyright 2018, The Royal Society of Chemistry. **i)** A self-powered electronic skin for measurement of uric acid, urea, glucose, and lactate with piezoelectric-enzymatic-reaction coupling. Reproduced with permission (Han et al., 2017). Copyright 2017, American Chemical Society.

lactate and cardiac signals, hence provided simultaneous measurements with both sensors to gain insights regarding cardiac health, human performance, and exertion levels. Fig. 3e shows a multi-analyte eyeglass for amperometric and potentiometric detection of lactate and potassium, respectively (Sempionatto et al., 2017). The printed sensors were integrated on the nose pads of the glasses and connected to the printed circuit boards on the different arms of the eyeglasses. This wireless lab-on-a-eyeglasses biosensor system demonstrated crosstalk-free measurement of metabolite and electrolyte levels.

Self-powered lactate and glucose sensing from perspiration eliminates the need for external power sources, amplification, and filtering, making it advantageous for the applications that require repeated recharging or *in vivo* operation. Fig. 3f shows an example of stretchable biofuel cells (BFCs) on a body-worn sock (Jeerapan et al., 2016). The BFC comprises a printed anode functionalized with LO_x and a redox material, and a cathode with a silver (I) oxide/silver redox couple. The self-powered biosensor increases its short circuit current with the increase in lactate concentration in sweat without a need for an applied bias, demonstrating a promising method for epidermal self-powered and energy harvesting applications. Similarly, Lu et al. demonstrated a self-powered and glucose, Na^+, and K^+ sensing system based on $NiCo_2O_4$ micro-supercapacitors (MSCs) (Lu et al., 2019). The MSC was used as power units to drive the nonenzymatic $NiCo_2O_4$/chitosan-based glucose and ion-selective Na^+ and K^+ sensors during a strenuous exercise (Fig. 3g).

Apart from glucose and lactate, there are other clinically relevant analytes in sweat, such as ethanol, uric acid, and urea. Overconsumption of alcohol contributes to the emergence of various health complications such as cardiovascular diseases, stroke, and liver cirrhosis (Campbell et al., 2018). Similarly, uric acid and urea are linked with hypertension, diabetes, cerebral infarction, renal insufficiency, and nervous system infection (Singh et al., 2008; Zhu and Cao 2012). Therefore, monitoring of these indicators is crucial in clinical settings from therapeutics to diagnostics. Real-time measurement of ethanol has been introduced by Hauke et al. using a skin-worn integrated device (Fig. 3h) (Hauke et al., 2018b). The device comprises an iontophoretic sweat stimulation, fluid handling, and ethanol sensing parts. The ethanol sensor was fabricated by drop-casting alcohol oxidase (AO_x), BSA, and chitosan on the sensing electrode. The reaction between ethanol and AO_x generated hydrogen peroxide as a byproduct, which was transduced by the platinum electrode. The authors demonstrated a significant correlation between blood and sweat ethanol concentration and reported a blood-to-sweat lag time due to the complex pharmacokinetics of ethanol in the body. Lastly, Han et al. developed a self-powered electronic skin for uric acid, urea, lactate, and glucose (Han et al., 2017). The self-powering and sensing mechanism is based on the coupling between enzymatic reactions of uricase, urease, GO_x, and LO_x, and piezoelectric effect zinc oxide nanowires (Fig. 3i). The study demonstrated real-time self-powered operation of the electronic skin during a running exercise, enabling simultaneous energy harvesting and sensing on flexible substrates.

The overall system architecture of the electrochemical wearable systems consists of an analog front-end circuit (AFE), a microprocessor (MCU) for data collection, processing, and transmission, and an energy management circuit. Amperometric sensors with two or three electrodes require a more complex AFEs for biasing the electrodes and reading current output (Imani et al., 2016b). Commercial potentiostat AFEs consist of a differential input amplifier and a programmable gain trans-impedance amplifier for biasing the electrodes at a constant voltage. Potentiostats enable current reading on the orders of pA to mA and have the capability of carrying out various electrochemical techniques, such as chronoamperometry and cyclic voltammetry. For instance, the wearable system in Fig. 3d used an LMP91000 potentiostat, which was controlled by a CC2541 BLE system-on-chip for data processing and communication (Imani et al., 2016a). The data was transmitted to a PC via BLE 4.0. The system used a button cell battery (3 V, 220 mAh) and a boost converter for energy management. The total current draw of the wearable system was 5 mA and consumed 15 mW in active mode. The system in Fig. 3e used a similar microcontroller (MCU) and AFE and reported 1.6 mA current draw with 100 mAh lithium-ion rechargeable battery during continuous operation (Sempionatto et al., 2017). In another study, Xu et al. demonstrated an NFC powered wearable glucose sensing system (Xu et al., 2019). The system included an NFC chip (NT3H2111, NXP Semiconductor) for power delivery and data transmission with a cellphone. The NFC chip was used to power the MCU (MSP430FR5959, TI) and potentiostat (LMP91002, TI). The MCU included a 12 bits ADC for digitization of output of the potentiostat, which was stored in the EEPROM of the NFC chip. The data was then wirelessly transmitted to a smartphone using a coiled antenna at 13.56 MHz and displayed on an Android app.

When the developments in the past few years are considered, the wearable systems for metabolite sensing have moved from just tattoo-based flexible sensors without signal conditioning circuitries to more complex wireless systems. The integrated, wireless systems included fluid handling channels for analyte sensing (Martin et al., 2017) as well as biofuel- and solar-powered autonomous monitoring (Jeerapan et al., 2016; Zhao et al., 2019).

2.2.2. *pH and electrolytes*

Regulation of pH in the human body has a crucial role in maintaining physiological homeostasis as the activity of most enzymatic reactions are dependent on pH. Body pH is determined by the dissociation of organic acids into H^+ ions in living cells. Any fluctuations in acid-base balance in the body may contribute to the development of fatigue and other metabolic diseases (Aoi and Marunaka 2014). Longitudinal monitoring of acid-base levels of the body may provide insights on ongoing disorders, such as metabolic and respiratory acidosis/alkalosis. Therefore, pH sensing has been an extensively researched field of wearable sensors. Fig. 4a demonstrates a roll-to-roll printed wearable electrochemical sensor for detecting pH, K^+, and Na^+ (Bariya et al., 2018b). The pH sensing was achieved by the functionalization of the sensing electrodes with ion-sensitive polymeric layers. The flexible pH sensor was interfaced with a custom PCB for measurement of the potential change on the sensing electrode with respect to the reference electrode. In another study, Pal et al. designed a wearable bandage for the measurement of pH changes using impedimetric analysis (Fig. 4b) (Pal et al., 2018). The bandage included an omniphobic paper, comprising a screen-printed electrode pairs with a polyaniline emeraldine salt (PANI-ES)-silver microflakes. Based on the concentration of H^+ in the surrounding environment, PANI underwent a reversible chemical reaction between its oxidized and reduced states, leading to an impedance change between the electrode pairs. Integration of the sensor with a miniaturized impedance analyzer atop enabled real-time wireless assessment of pH. In a different study, Kassal et al. demonstrated an optical approach for the quantification of pH within a narrow range (pH 6 to 9) Fig. 4c (Kassal et al., 2017). The skin-worn bandage included a polyurethane-based hydrogel containing a pH-sensitive indicator. The pH indicator dye changed its absorbance at 534 nm as the pH of the buffer solution varied. The sensor was coupled with a LED (527 nm) and a photodiode for the measurement of the reflected light. The intensity of the reflected light decreased as the indicator dye changed its degree of deprotonation. The wearable system used an RFID reader for powering and data transmission as well as a current source and a transimpedance amplifier for driving the LED and measuring the photodiode current. Curto et al. demonstrated a wearable barcode-like microfluidic patch integrated with pH-sensitive ionic liquid polymer gels (Curto et al., 2012). Incorporation of pH-sensitive dyes with varying pKa values into the ionogels enabled real-time analysis of sweat (Fig. 4d). pH measurement was made by capturing pictures of the barcode at different time intervals with a camera and outputting a single pH value by equally weighing the contribution of each pH-sensitive dye. The addition of reference colors onto the microfluidic patch eliminated the effect of ambient light variations.

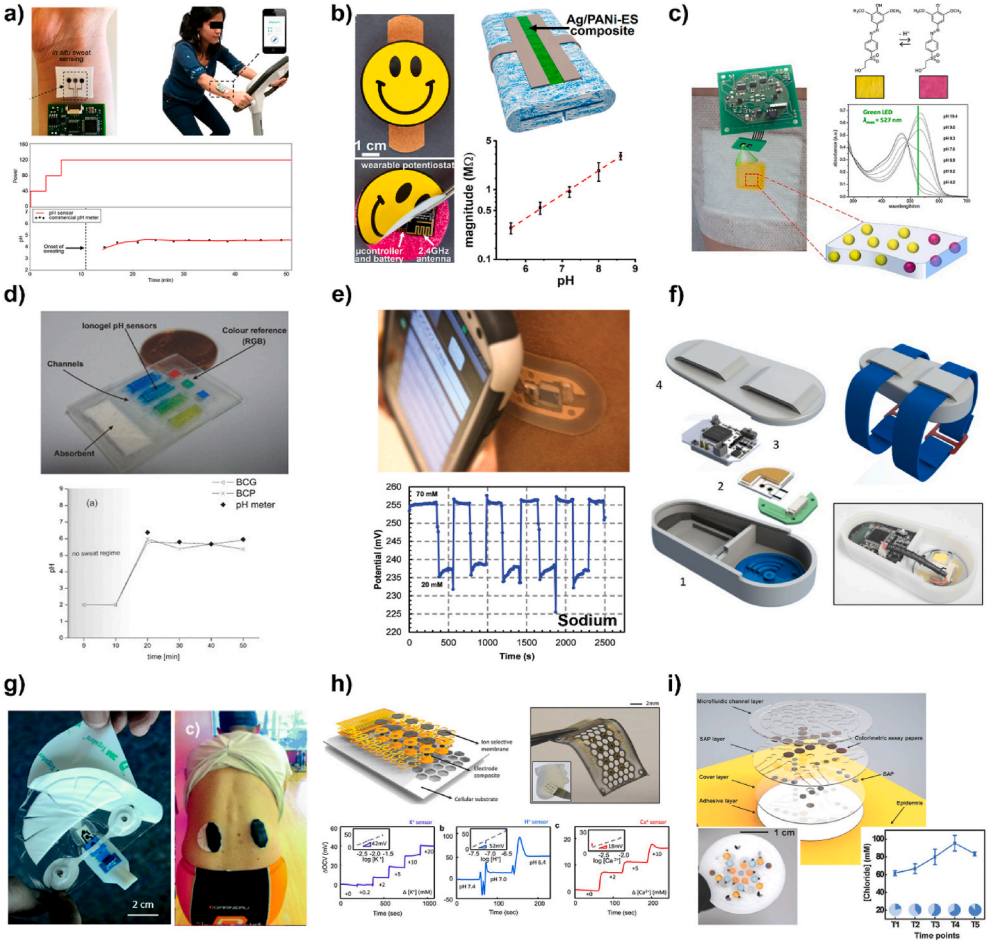

Fig. 4. Examples of electrochemical, optical, and colorimetric wearable sensors for electrolyte sensing. **a)** A roll-to-roll printed electrode arrays for pH, K^+, and Na^+ sensing. Reproduced with permission (Bariya et al., 2018b). Copyright 2018, American Chemical Society. **b)** An omniphobic paper-based smart bandage for pH sensing. Reproduced with permission (Pal et al., 2018). Copyright 2018, Elsevier. **c)** A smart bandage for optical monitoring of pH. Reproduced with permission (Kassal et al., 2017). Copyright 2017, Elsevier. **d)** A wearable chemical barcode microfluidic platform for pH sensing. Reproduced with permission (Curto et al., 2012). Copyright 2012, Elsevier. **e)** An RFID patch for Na^+ sensing. Reproduced with permission (Rose et al., 2015). Copyright 2015, IEEE. **f)** SWEATCH wearable Na^+ sensing device. Reproduced with permission (Glennon et al., 2016). Copyright 2016, John Wiley and Sons. **g)** A wearable patch for monitoring of Na^+ and K^+. Reproduced with permission (Alizadeh et al., 2018). Copyright 2018, The Royal Society of Chemistry. **h)** A thin elastomeric patch with open cellular designs for pH, K^+, Ca^{2+} sensing. Reproduced with permission (Lee et al., 2017b). Copyright 2017, WILEY-VCH Verlag GmbH & Co. **i)** A microfluidic patch with superabsorbent valves for time-sequenced colorimetric monitoring of Cl^-. Reproduced with permission (Kim et al., 2018b). Copyright 2018, WILEY-VCH Verlag GmbH & Co.

The pH monitoring wearable systems employed different AFEs based on their pH transduction techniques (*i.e.,* potentiometric, impedimetric, optical, or colorimetric). The potentiometric sensors included an instrumentation amplifier and filtering stages (1 Hz) to minimize the common-mode interferences and high-frequency noise (Gao et al., 2016a). The impedimetric sensor included an impedance analyzer (AD5933, Analog Devices Inc.) for pH analysis at 100 Hz (Pal et al., 2018). In contrast to electrochemical methods, the optical and colorimetric sensors measured pH by evaluating the change in light intensity and color of the sensor using a photodetector and image analysis, respectively.

Apart from H^+ sensing, wearable systems for real-time analysis of other ions have been developed. Fig. 4e demonstrates an RFID sensor patch for monitoring of sweat Na^+ levels (Rose et al., 2015). The flexible patch used ion-selective electrodes (ISEs) with paper microfluidics for potentiometric measurement of electrolyte levels. The patch included a coiled antenna for the inductive powering of an RFID transponder chip. The chip measured the potential difference between two ion-selective electrodes. The transfer of the pH data to the aggregator was done via NFC. The patch operated up to seven days and enabled battery-free detection of other ionic solutes in sweat. In contrast to the battery-free operation, Fig. 4f-g shows battery-powered, wireless wearable devices for real-time Na^+ or K^+ measurement (Alizadeh et al., 2018; Glennon et al., 2016). The wearable systems included an absorbent pad for extended sweat collection, pH-sensitive ISEs as well as a miniaturized Shimmer™ board for the differential voltage measurement and wireless transmission. The sweat patch in Fig. 4g used magnetic connectors between the sensor and the electronic module to minimize the motion artifact noise in potentiometric measurements during the human trials, which was necessary for signals with high fidelity. Lee et al. demonstrated a chemical sensing patch with an open cellular design comprising a multiplexed array of sensing electrodes for H^+, K^+, and Ca^{2+} monitoring (Lee et al., 2017b). The thin patch enabled an intimate contact with the skin surface without mechanical irritation and provided a spatiotemporal mapping of the target electrolytes on the skin surface (Fig. 4h). Finally, Kim et al. developed a microfluidic device for colorimetric detection of chloride (Cl^-) ions (Kim et al., 2018b). The flexible and skin conformable device comprised microchannels, isolated reservoirs, and super-absorbent polymer valves for time-sequenced discrete sampling as well as measurement of Cl^- in sweat (Fig. 4i). The chloride assay relied on competitive chelation between mercury (II), ferrous (II) with a chelating agent, 2,4,6-tris(2-pyridyl)-s-triazine, yielding blue assay color with increased chloride concentration. The quantitative analysis of the Cl^- was done using digital images of the microfluidic patch.

The wearable systems for pH and electrolyte monitoring included much broader signal transduction alternatives (electrochemical, optical, and colorimetric) compared to the metabolite sensing. While the colorimetric systems are simple to fabricate, they may not be the first choice for the applications that require extended electrolyte monitoring due to its infrequent sampling and lower sensor resolution. The preconditioning circuitry and signal processing for electrochemical electrolyte sensing are more straightforward than that of the optical systems. Therefore, they have been widely used in various applications, ranging from exercise physiology in sports medicine to cystic fibrosis detection in clinical medicine.

2.2.3. Oxygen

Oxygen has critical roles in the human body, such as in metabolism (energy production via oxidative phosphorylation), biochemistry (reactive oxygen species and gene transcription), and pathology (determining the condition and function of tissue structure). Its excess leads to inflammation and tissue damage, while its shortage induces severe tissue damage in the heart and brain (Wagner 2008). Due to its critical importance, various optical methods (photoplethysmography and pulse oximetry) have been developed to quantify its concentration in the body.

Photoplethysmography (PPG) is an optical method that relies on a light source and a detector for the measurement of changes in blood volume (Kamal et al., 1989). Beating of the heart causes fluctuations in the blood volume of arteries and changes the light attenuation through blood and tissue. The PPG sensors measure the change in the light attenuation using light-emitting diodes (LEDs) or photodiodes (PDs). Similarly, pulse oximeter relies on light absorption differences of oxygenated (HbO_2) and deoxygenated hemoglobin (Hb) and provides an estimation of the arterial oxygen saturation (SpO_2) using two PPG signals from specific regions of the light spectrum (green-red or red-infrared) (Bowes et al., 1989). PPG and pulse oximetry give critical information about cardiovascular health by measuring heart rate, blood pressure, blood oxygenation, and heart rate variability (Allen 2007).

In this regard, organic optoelectronic devices have been reported for the development of flexible and stretchable wearable optoelectronic systems. Fig. 6a shows an ultra-flexible organic photonic skin for measurement and a digital display of pulse oximeter information (Yokota et al., 2016). The flexible photonic skin was made up of organic LEDs (red and green) and a PD. Due to the soft nature of polymers and prestraining of the underlying substrate, the optical devices maintained their optoelectronic characteristics under repeated stretching cycles and yielded low noise PPG signals due to its excellent adhesion with skin. Khan et al. designed a reflectance oximeter array for the measurement of SpO_2 and spatial 2D oxygenation (Khan et al., 2018). The flexible patch utilized screen-printing and blade coating for the fabrication of 2×2 pixels of organic LEDs (612 nm and 725 nm) and 8 pixels of organic PD devices on flexible substrates (Fig. 6b). The study showed single-point PPG, heart rate, SpO_2 measurement. Real-time 2D tissue oxygenation during an ischemic event was also demonstrated. This function enabled the measurement of localized tissue oxygenation when the pulsatile arterial blood signal of PPG was low. In another study, Han et al. designed an organic ambient light oximeter (ALO) for the measurement of PPG and SpO_2 from the index finger (Fig. 6c) (Han et al., 2020). The optoelectronic device used only PDs, eliminating the need for any light source and LED drivers. Since the absorbance spectrum of organic polymers is broad, the ALO used flexible filters on top of PDs for selective detection of green (525 nm), red (610), and near-infrared lights (740 nm) with negligible spectral overlap. Overall, organic optoelectronic devices are skin-conformable and can be fabricated to cover large areas on the skin surface. However, due to the air stability of organic devices, the operation of the wearable systems in ambient conditions is limited to orders of a few days.

Inorganic optoelectronic devices are air-stable and reliable; therefore, they have been widely used in wearable sensors for oxygen monitoring. Fig. 6d shows a skin-worn optoelectronic system for optical interrogation of the skin (Kim et al., 2016). The wearable device is skin conformable and uses magnetic inductive coupling and near-field communication for powering the LED (950 nm) and transmission of the PPG signal. In another study, Chung et al. designed wireless chest and limb patches for the physiological monitoring of neonatal and pediatric patients (Fig. 6e) (Chung et al., 2020). Both patches employed flexible PCBs with stretchable interconnects and batteries, which were entirely encapsulated in a flexible silicone material. The chest patch provided sensory data such as the electrocardiogram (ECG), respiratory rate, and seismocardiogram (SCG), whereas the limb patch measured PPG, SpO_2, and temperature. The time-synchronized operation of two patches enabled the extraction of pulse arrival time, pulse transit time, and systolic blood pressure from ECG, SCG, and PPG signals, which may not be easily obtainable from a single device. Similarly, Zhang et al. demonstrated an optical system for extended measurement of tissue oxygen saturation levels ($rStO_2$) using microscale inorganic light-emitting diodes (μ-LEDs) and photodetector (μ-IPD) (Zhang et al., 2019a). The system included an injectable sensing filament with integrated μ-LEDs (540 nm and 625 nm) and μ-IPD, as shown in Fig. 6f. Similar to other oximeters, the μ-LEDs operated in a time-multiplexed fashion, and the μ-IPD measured the backscattered light by the surrounding tissue and vasculature. Even though the fabrication of the optical sensor included complicated fabrication steps, the use of μ-LEDs and μ-IPD along with a miniaturized wearable system enabled localized tissue oxygenation measurements in deep tissues, which would not be easily achieved by commercial inorganic LEDs and PDs.

The instrumentation for wearable optical systems includes a microcontroller, a wireless transmission module as well as LED drivers, amplifiers, and filters for sequential driving of LEDs, amplification of photodiode current, and elimination of low and high-frequency noise (Webster 1997). For mobile applications, fully integrated AFEs that house an LED driver and a low-noise receiver channel with an integrated ADC have commonly used. For instance, the reflective oximeter array and ambient light oximeter in Fig. 6b and c used an integrated AFE (AFE4490, TI) with external analog switches for the sequential drive of an array of OLEDs and read out from the OPDs. The optical AFE was controlled by an Arduino Uno microcontroller (500 Hz sampling), and the data was collected using a USB interface. In another study in Fig. 6d, the wireless optoelectronic system used a bare die NFC chip (SL13A, ams AG) to measure PPG signals and heart rate using an LED and a photodetector. The photodetector current was amplified by a transimpedance amplifier and sampled by 10-bit ADC at 25 Hz, which was satisfactory for the detection of systolic and diastolic peaks in the PPG signal. An NFC-enabled smartphone was used for powering the system and data transmission (13.56 MHz, ISO 15693) from the NFC chip. The power management unit of the NFC chip provided the external biasing for the LED and photodetector. The wireless system in Fig. 6e consisted of a time-synchronized operation of the wearable chest and limb units for health monitoring in pediatric and neonatal intensive-care units. The limb unit included an integrated pulse oximeter AFE (MAX30101, Maxim Integrated) for the measurement of dual-wavelength PPG using on-chip LEDs (660 nm and 880 nm) and a photodiode. A BLE SoC (nRF52832, Nordic Semiconductor) was used for sampling the PPG signals (100 Hz), processing, and data logging to a computer. The post-processing of the collected PPG data included band-pass filtering (0.8–8 Hz), onset and beat detection algorithms, as well as FFT, red/IR ratio density estimation and SpO_2 calculation. Battery-powered and wireless-powering operation of the system was demonstrated for alternative health monitoring options in intensive-care units.

When NFC and BLE-operated wireless optoelectronic systems are compared, the wireless-powering eliminates the need for battery use; however, the maximum power that can be delivered to the system is limited by the orientation and distance of the NFC device relative to the wireless coil. In wearable optical systems, on-board signal processing and optimization of the critical parameters of wireless transmission and LEDs, such as duty cycling, LED-detector distance, sampling frequency, clock frequency, and transmission of physiological data in pockets, determine the total power consumption of wearable optical systems in the presence of motion artifacts (Pelaez and Villegas 2007; Rhee et al., 2001; Tamura 2019).

2.2.4. Other chemical biomarkers

In addition to metabolites and electrolytes, other biomarkers, and chemical substances, such as hormones, and vitamins, heavy metals, and drugs, emerge in sweat that can be used towards stress assessment, doping control, and health and disease monitoring (Gao et al., 2016b; Parlak et al., 2018; Sempionatto et al., 2020b; Tai et al., 2020). Fig. 5a

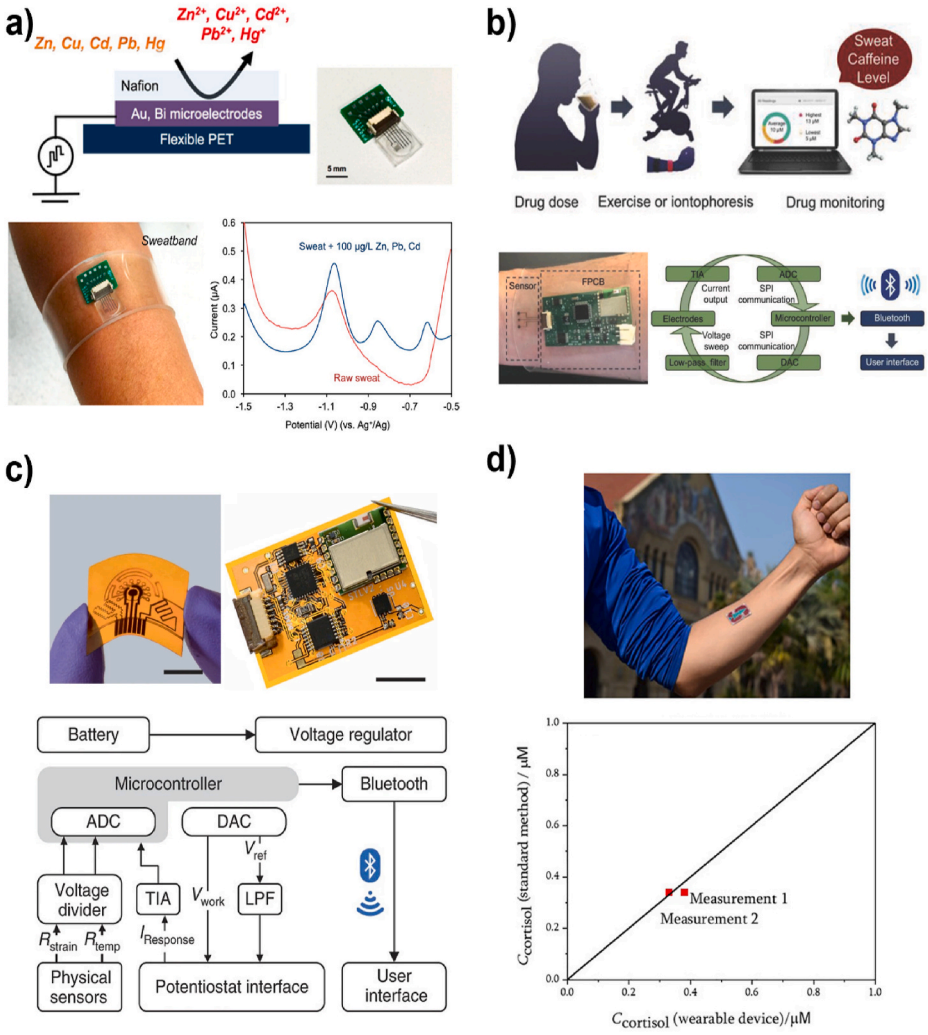

Fig. 5. Examples of wearable sensors for the detection of other analytes in sweat. a) A flexible multiplexed array for detection of Zn, Cd, Pb, Cu, and Hg. Reproduced with permission (Gao et al., 2016b). Copyright 2016, American Chemical Society. b) A flexible sweatband for caffeine monitoring. Reproduced with permission (Tai et al., 2018). Copyright 2018, WILEY-VCH Verlag GmbH & Co. c) A laser-engraved graphene-based sensor for uric acid, tyrosine, temperature, and respiration rate monitoring. Reproduced with permission (Yang et al., 2020). Copyright 2020, Springer Nature. d) An organic electrochemical transistor modified with molecularly imprinted polymer for cortisol sensing. Reproduced with permission (Parlak et al., 2018) Copyright 2018, Creative Commons Attribution Noncommercial License 4.0.

shows a flexible multiplexed array for heavy metal detection in sweat. The multiplexed array comprises a bismuth (Bi) and a gold (Au) working microelectrode (Gao et al., 2016b). The study used electrochemical square wave anodic stripping voltammetry (SWASV) for the detection of cadmium (Cd), lead (Pb), and zinc (Zn) on the Bi microelectrode. The Au microelectrode was used for the detection of lead, copper (Cu), and mercury (Hg). On-body trials of the flexible array with sweat demonstrated the use of the wearable sensor for gaining insightful information on heavy metal exposure. In another study by Javey's group, a wireless system was developed for real-time monitoring of caffeine in sweat upon a caffeine intake (Tai et al., 2018). The flexible sensor was modified with carbon nanotube/Nafion solution, and the electrochemical detection of caffeine was made via differential pulse voltammetry (DPV). The DPV parameters were controlled with a microcontroller by adjusting the voltages on the reference and working electrodes using an external digital-to-analog converter. The current on the working electrode was converted into voltage using a transimpedance amplifier, digitized by an external ADC through SPI protocol, and sent to the data aggregator via Bluetooth (Fig. 5b). The wearable device measured the presence of caffeine in iontophoresis and exercise-induced sweat and revealed the potential of using this platform towards clinical pharmacology and precision medicine.

In another study, Yang et al. demonstrated a laser-engraved wearable sensor for uric acid (UA) and tyrosine (TYR) detection in sweat for gout and fitness analysis (Fig. 5c) (Yang et al., 2020). The chemical sensing of UA and TYR was done using laser-engraved graphene due to its high surface area and electrochemical activity. A similar AFE design reported in Fig. 5b was used for the measurement of UA and TYR in sweat via the DPV method. On-body sweat and serum measurements revealed the correlation of uric acid in healthy subjects and patients with gout. In another study, Parlak et al. fabricated an organic electrochemical transistor (OECT) for cortisol sensing towards stress evaluation (Fig. 5d) (Parlak et al., 2018). Detection of cortisol was done by covering the semiconducting channel of the OECT with a cortisol-selective molecularly imprinted polymer. In the presence of the analyte, the ion exchange between the sensing medium and the transistor channel was prevented, leading to a reduced source-drain current of the OECT. The authors demonstrated real-time and selective measurement of cortisol in sweat with the wearable OECT during an exercise.

The detection of heavy metals and drugs in sweat required complex electrochemical methods, such as SWASV or DPV. System-level implementation of these methods were similar to the other electrochemical methods (*i.e.*, chronoamperometry), only differed in the regulation of reference and working electrode voltages using an external DAC to set electrochemical parameters (*i.e.*, frequency, potential, and pulse parameters).

3. Wearable biophysical sensing

3.1. Sweat rate

Sweat rate is an important physical parameter for the diagnosis and

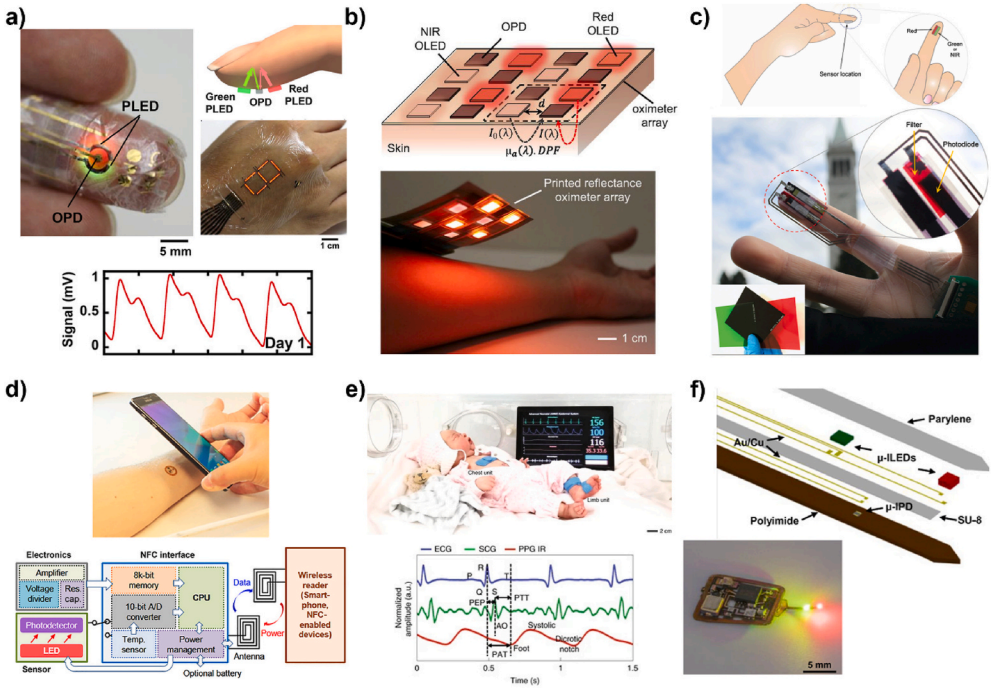

Fig. 6. Examples of wearable optical sensors for the detection of oxygen. a) Smart e-skin system comprising ultra-flexible polymer light-emitting diodes (PLEDs) and an organic photodetector (OPD). Reproduced with permission (Yokota et al., 2016). Copyright 2016, Creative Commons Attribution 4.0 International License. b) A reflective oximeter with an array of red and NIR LEDs and OPDs. Reproduced with permission (Khan et al., 2018). Copyright 2018, Creative Commons Attribution 4.0 International License. c) An ambient light oximeter (ALO) with printed OPDs. Reproduced with permission (Han et al., 2020). Copyright 2020, WILEY-VCH Verlag GmbH & Co. d) A battery-free, wireless, epidermal optoelectronic system. Reproduced with permission (Kim et al., 2016). Copyright 2016, Creative Commons Attribution 4.0 International License. e) A soft, wireless chest and limb units for physiological monitoring of neonatal and pediatric patients. Reproduced with permission (Chung et al., 2020). Copyright 2020, Springer Nature. f) A miniaturized, wireless oximeter with microscale LEDs (μ-LEDs) and a microscale inorganic photodetector (μ-IPD). Reproduced with permission (Zhang et al., 2019a). Copyright 2019, Creative Commons Attribution 4.0 International License.

evaluation of excessive sweating and monitoring of dehydration status (Atkins and Butler 2002; Brake and Bates 2003). Dehydration causes physical, mental, physiological loss in performance and is commonly associated with heat-induced cramps, fatigue, dizziness, or strokes (Casa et al., 2000; Gopinathan et al., 1988; Leithead and Lind, 1964). Therefore, sweat rate sensors have been included in the development of wearable sensors. For example, Fig. 7a shows a simple approach for the detection of sweat volume. The wearable device employed a soft PDMS channel and a Teflon tube for collection and guiding of sweat into the microchannel. Sweat volume was measured by determining the distance traveled by the fluid in the channel over the duration of the testing. The sweat rate was then calculated by taking the time derivative of the sweat volume (Liu et al., 2016). In a different study, a microfluidic channel with a pair of electrodes was constructed for measurement of sweat rate over a wide dynamic range of flow rates (Fig. 7b) (Francis et al., 2019). Once sweat was captured through an opening, it formed a droplet in the hydrophobic channel, which electrically shorted the bottom electrode (gold electrode) and top electrode (Nickel conductive wicking material) and resulted in a current spike under a constant DC bias. The continuous sweat rate sensing was ensured by a mesh-like conductive top electrode, which removed the collected sweat away from the sensing area and enabled the formation of a new droplet between electrodes. The sweat rate was estimated by dividing the droplet volume by the time between two consecutive current spikes. However, the deposition of salt at the inlet of the device distorted the acquired signal and limited the lifetime of the sensor.

Similarly, Javey's group demonstrated impedance-based, wearable sweat rate sensing systems with integrated microfluidic channels, as shown in Fig. 7c and d. Both studies incorporated microfluidic channels for extended sweat collection and sweat rate measurement. For instance, the wireless system in Fig. 7c comprises a Na^+ sensor and a spiral impedance sensor with a microfluidic channel for real-time sweat rate measurement (Nyein et al., 2018b). An impedance analyzer (AD5933, Analog Devices) was used for the measurement of impedance at 100 Hz. As the sweat filled out the microfluidic channel, the admittance of the sensor increased because of an increased sweat volume and total ion concentration. Na^+ concentration in the microfluidic channel contributed to the admittance change; therefore, a Na^+ sensor was included at the entrance of the microfluidic channel for measurement of Na^+ levels. Real-time estimation of the sweat rate was performed using both the admittance and Na^+ concentration. In this study, the output of this sensor was influenced by both sweat ion composition and sweat volume; therefore, an improved impedimetric sweat rate sensor was proposed by the same group (Yuan et al., 2019). The sensor consisted of an interdigitated electrode and a serpentine-shaped microfluidic layer. Each time the collected sweat in the microfluidic channel encountered a new electrode finger, the admittance between electrodes gave a sharp jump. The sweat rate was calculated by dividing the total fluid volume between electrodes by the time between admittance jumps. Comparable devices have been reported which integrate the admittance-based sweat rate quantification with paper microfluidics and conventional screen printing techniques (Yokus et al., 2020a). In another study by Rogers's group, a fully integrated battery-free, reusable, NFC integrated sweat rate system was reported (Fig. 7e) (Kim et al., 2018a). The wearable system included a microfluidic channel with integrated electrodes for impedimetric sweat rate sensing, and an NFC electronic module for powering, energy harvesting, and data communication. An NFC compatible device (*i.e.*, smartphone) wirelessly powered the NFC module. On power-up, the system applied a 5 kHz waveform to the electrodes in the microfluidic channel, causing a current to flow. Sweat flow in the microchannel changed the resistance between electrodes and attenuated the magnitude of the applied waveform. The waveform was rectified and processed by a microcontroller and sent back to the smartphone over the NFC link. Utilization of a fully integrated fabrication approach along with a re-attachable NFC electronic system via small magnets facilitated real-time monitoring of sweat loss in various exercise conditions. Overall, the integration of electrical impedance sensing with sophisticated fabrication techniques, unique microchannel designs, fluid wicking materials, and miniaturized electronics enabled accurate and real-time detection of sweat rate information.

Alternative wearable sweat rate sensing approaches have also been reported. Fig. 7f shows a skin-like waterproof microfluidic sensor

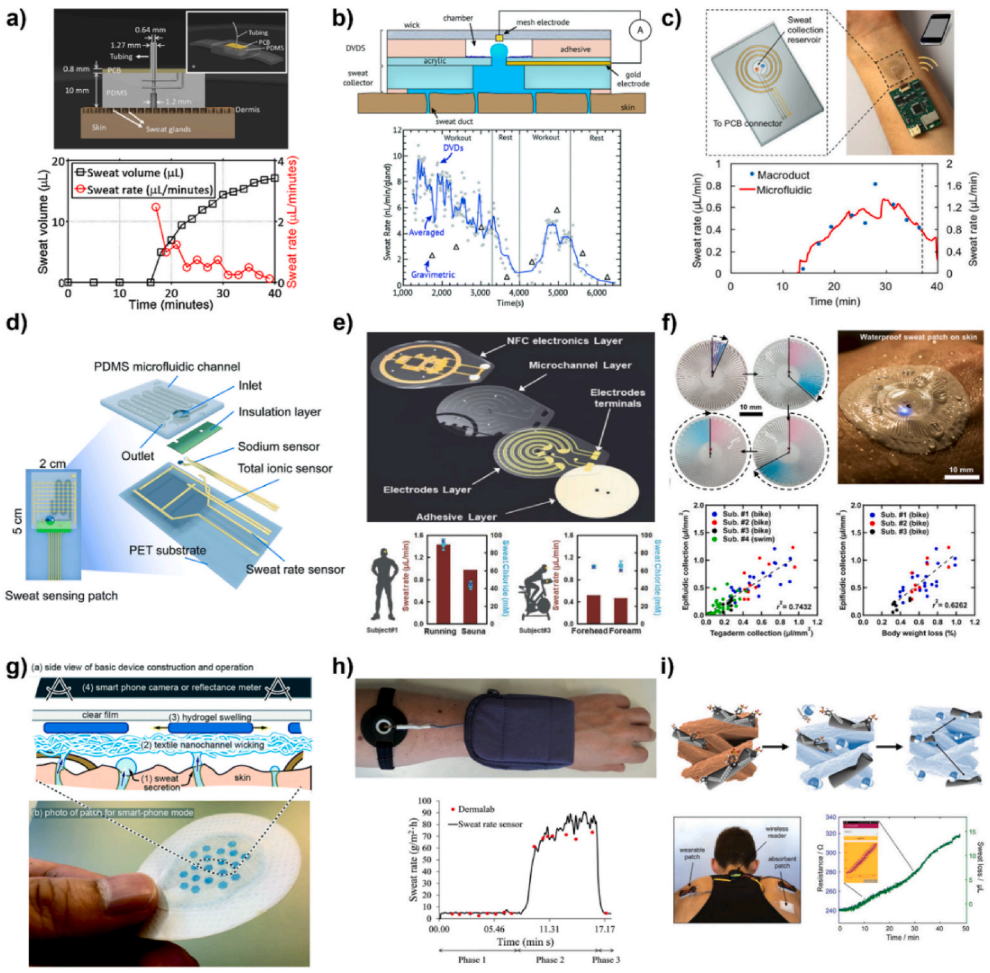

Fig. 7. Examples of wearable sweat rate sensors. a) A wireless sweat volume and conductivity sensor. Reproduced with permission (Liu et al., 2016). Copyright 2016, Elsevier. b) A digital volume dispensing system for sweat rate measurement. Reproduced with permission (Francis et al., 2019). Copyright 2019, The Royal Society Chemistry. c) A wearable wireless sweat patch for Na^+ and sweat rate sensing. Reproduced with permission (Nyein et al., 2018b). Copyright 2018, American Chemical Society. d) A multi-model sweat sensing patch for measurement of Na^+, sweat rate, and total ionic concentration. Reproduced with permission (Yuan et al., 2019). Copyright 2019, The Royal Society Chemistry. e) A battery-free, wireless microfluidic system for sweat rate and loss monitoring. Reproduced with permission (Kim et al., 2018a). Copyright 2018, WILEY-VCH Verlag GmbH & Co. f) A waterproof, epidermal microfluidic sweat patch for virtual assessment of sweat loss in an aquatic environment. Reproduced with permission (Reeder et al., 2019). Copyright 2019, Creative Commons Attribution 4.0 International License. g) A sweat volume monitoring patch with swellable hydrogels. Reproduced with permission (Zhao et al., 2020a). Copyright 2020, The Royal Society Chemistry. h) A wearable sweat rate sensor based on the diffusion of the water vapor evaporated from the skin. Reproduced with permission (Salvo et al., 2018). Copyright 2018, Elsevier. i) A wearable and wireless sweat rate monitoring system based on chemiresistors. Reproduced with permission (Parrilla et al., 2019b). Copyright 2019, WILEY-VCH Verlag GmbH & Co.

laminated on the skin for sweat capture and colorimetric assessment of sweat loss in aquatic environments (Reeder et al., 2019). The inlet of the microfluidic channel houses a colorimetric reagent for visual assessment of the extent of sweat filling in the microfluidic channel (total volume ~60 μL). The study reported a good correlation between the sweat collected by the microfluidic device and other sweat loss evaluation techniques such as absorbent patch and whole-body weight loss measurements during swimming and biking exercises. In another study, a skin-worn device with swellable hydrogels were designed for monitoring sweat rate (Zhao et al., 2020a). Hexagon-shaped hydrogels increased their surface area with the absorption of sweat (Fig. 7g). The increase in the geometry, thus the sweat volume, was measured by taking an image of the hexagon or by measuring the optical reflectance of a local area (white-colored wicking fabric) as the blue-colored hydrogel slowly covered it upon sweat absorption.

Other wearable sweat rate sensors based on the diffusion of the water vapor from the skin surface (Fig. 7h) and chemiresistors (Fig. 7i) were explored. The first wearable system relied on differential measurements from humidity and temperature sensors to calculate the weight of evaporated vapor in a sealed chamber close to the skin surface and enabled real-time sweat rate and sweat loss monitoring (Salvo et al., 2018). The latter study used single-walled carbon nanotube (SWCNTs) based ink on paper substrates for real-time measurement of the sweat loss (Parrilla et al., 2019b). Upon sweat absorption, the cellulose fibers swelled and increased the distance between the SWCNTs, thus the resistance. The integration of the chemiresistors with a wireless system provided an inexpensive and disposable sweat sensing approach for real-time dehydration monitoring.

Wearable systems employed various approaches for the estimation of sweat rate, such as impedance- and water vapor-based assessment, visual evaluation of microchannels as well as volumetric expansion of hydrogels upon sweat absorption. The impedance-based approaches were commonly integrated with microfluidic channels and their associated electronics for real-time assessment of sweat loss. The sweat rate calculation based on sweat vapor is robust to variation in sweat composition and can provide accurate sweat rate measurement. In contrast to the previous approaches, the techniques that relied on visual assessment may require user intervention for discrete and temporal assessment of local sweat rates.

3.2. Temperature

Core body temperature is a significant health indicator in addition to heart rate, blood pressure, and oxygenation. It varies due to endogenous (measurement site, circadian and menstrual rhythms, fitness, and aging) and exogenous factors (environment, diet, and lifestyle) (Kelly 2006, 2007). Variation from the homeostatic body temperature (≈37 °C) gives insights about metabolism, thermoregulation, viral/bacterial infections, inflammation, and pathological conditions, which makes the body temperature as an essential diagnostic indicator (Clark 1984; Kelechi and Michel 2007).

Current wearable temperature sensing systems employed resistive and colorimetric methods with varying levels of integration of electronics towards health and wellness monitoring. Fig. 8a and b show examples of flexible resistive temperature sensors for skin temperate monitoring (Nakata et al., 2017; Yamamoto et al., 2017). The sensors

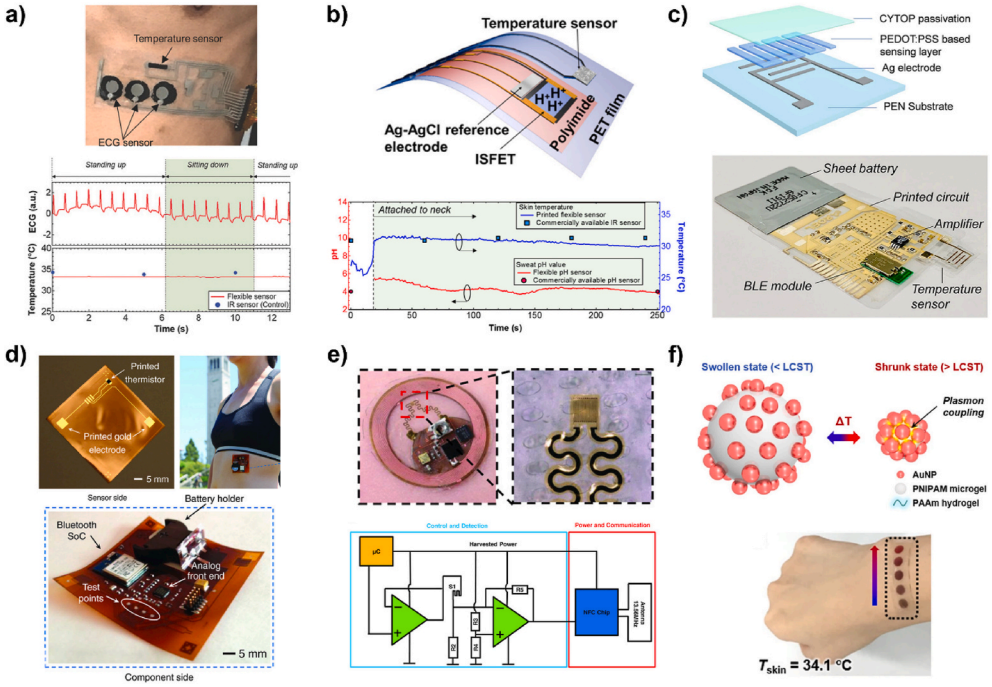

Fig. 8. Examples of wearable temperature sensors. a) A flexible healthcare patch with temperature and ECG sensing capabilities. Reproduced with permission (Yamamoto et al., 2017). Copyright 2017, WILEY-VCH Verlag GmbH & Co. b) A wearable, flexible sensor with pH and temperature sensors. Reproduced with permission (Nakata et al., 2017). Copyright 2017, American Chemical Society. c) A flexible wireless temperature-sensing platform with a printed temperature sensor. Reproduced with permission (Wang et al., 2020). Copyright 2020, Creative Commons Attribution 4.0 International License. d) A wireless wearable sensor patch for ECG and temperature sensing. Reproduced with permission (Khan et al., 2016). Copyright 2016, WILEY-VCH Verlag GmbH & Co. e) An epidermal wireless thermal sensor (eWTS) with a thin and soft thermal sensing/actuating component. Reproduced with permission (Krishnan et al., 2018). Copyright 2018, WILEY-VCH Verlag GmbH & Co. f) A thermoresponsive colorimetric temperature sensor with plasmonic gold nanoparticles in PNIPAM hydrogels. Reproduced with permission (Choe et al., 2018). Copyright 2018, Creative Commons Attribution 4.0 International License.

were made by screen-printing a mixture of carbon nanotube and poly(3, 4-ethylenedioxythiophene) polystyrene sulfonate (PEDOT:PSS) solution. However, the sensors exhibited sensitivity to humidity changes due to the hydrophilic nature of PSS (Benchirouf et al., 2016). Fig. 8c shows a fully flexible, wireless temperature sensing system based on PEDOT:PSS (Wang et al., 2020). The humidity variation of the temperature sensor was minimized by encapsulating the sensors with a fluorinated polymer. The flexible circuitry was realized by ink-jet printing silver ink on a PEN substrate. The system was able to perform on-site temperature reading, conditioning, and wireless transmission of the on-body temperature reading to a smartphone. In another study by Khan et al., a wearable sensor patch with continuous ECG and temperature sensing was demonstrated (Fig. 8d) (Khan et al., 2016). The study used a thermistor composed of nickel oxide nanoparticles mixed in polystyrene-butadiene binder. The resistance of the thermistor was sensed with a voltage divider network. After digitization of the temperature data, the information was sent to a host computer via Bluetooth for further processing.

Different from other wireless systems, Krishnan et al. reported a battery-free and NFC operated flexible system for thermal characterization of the skin (Krishnan et al., 2018). The system measured the blood perfusion, hydration, and trauma on the skin by measuring the thermal conductivity change of the skin with the Cr/Au temperature sensor. The overall system consisted of an inductive coil, a microcontroller, and its associated passive components for RF energy harvesting and data transmission (Fig. 8e). In a different study, Choe et al. demonstrated a cost-effective colorimetric temperature sensor for skin temperature monitoring. The colorimetric sensors were created by combining plasmonic gold nanoparticles with thermoresponsive poly (N-isopropyl acrylamide) (PNIPAM) hydrogels (Choe et al., 2018) (Fig. 8f). The volumetric change of PNIPAM hydrogels upon heating changes the plasmonic coupling between the nanoparticles, resulting in a red shift in its extinction spectra and a change in the RGB color values of the image of the sensor. By tuning the lower critical solution temperatures of the hydrogels, the authors created a colorimetric patch for spatial skin temperature mapping with a satisfactory temperature resolution (0.2 °C) and dynamic range.

In comparison to the resistive temperature sensors and thermistors, the colorimetric temperature sensing does not provide sufficient temperature resolution and accuracy for long-term monitoring. Benefits of flexible resistive temperature sensors and thermistors (miniaturization, simplicity of circuit design, and ease of integration with the skin) extended their uses to other exciting applications, such as estimation of the core body temperature (Zhang et al., 2016), calibration of the response of temperature-dependent biosensors (Gao et al., 2016a), and mitigating the risks of the formation of skin ulcers (Han et al., 2018).

4. Wearable systems with multimodal sensing

Skin-interfaced wearable biochemical systems provide insights on molecular-level changes in human performance and physiology. A comprehensive understanding of human physiology necessitates longitudinal monitoring of biochemical data in addition to biophysical and environmental information (Misra et al., 2019). The integration of biochemical sensors with other physical sensors, such as heart rate, SpO_2, sweat rate, and temperature, provides a wealth of information that may not be easily obtained from a single type of sensor (Table 2). These systems not only provide an overall assessment of health and performance by synthesizing and correlating the multisensory data but also enables other features, such as improving the accuracy of the diagnostic decision based on multiple sensor outputs and calibration of enzymatic sensors with pH and temperature sensors (Gao et al., 2016a; Imani et al., 2016a; Lee et al., 2017a; Nakata et al., 2017; Wiorek et al., 2020; Xu et al., 2019).

Recent studies have demonstrated the concept of multimodal sensing by integrating multiple sensing modalities into unified wireless platforms. Fig. 9a shows a wearable and wireless multiplexed biosensor system for measurement of glucose, lactate, pH, and temperature using a flexible sensor array (Yokus et al., 2020b). The auxiliary physical sensors could measure pH and temperature in physiological range and provide a real-time supplementary data that can be used for compensation of enzymatic loss of the biosensors. The flexible sensing array incorporated twelve working electrodes for simultaneous and multiplexed detection of glucose and lactate. Utilization of three multiplexers and potentiostats

Table 2
List of biochemical and biophysical sensors with their health applications.

Analyte or Signal	Health Application	References
glucose	diabetes, diet management	Moyer et al. (2012)
lactate	physical performance, anaerobic metabolism, Frey's syndrome, pressure ischemia	Derbyshire et al. (2012)
urea, uric acid, creatinine, ammonia	renal dysfunction	Tricoli and Neri (2018)
pH, sodium, chloride	acid-base balance, cystic fibrosis, dehydration, wound healing	(Cheuvront and Kenefick 2014; Dill et al., 1938; Gibson and Cooke 1959; Percival et al., 2014)
cortisol	stress monitoring	Torrente-Rodriguez et al. (2020)
ethanol	assessment of intoxication	Buono (1999)
zinc, copper, cadmium, lead, mercury	assessment of toxic metal exposure	Gao et al. (2016b)
electrocardiogram, heart rate, heart rate variability	cardiovascular and pulmonary diseases	(Agarwal et al., 2008; Sessa et al., 2018)
photoplethysmogram, SpO_2	hypertension, vascular aging, blood perfusion, hypovolemia, oxygenation	(Elgendi et al., 2019; Roederer et al., 2015; Yousef et al., 2012)
sweat rate	dehydration	Maughan and Shirreffs (2010)
temperature	hyperthermia, infection, inflammation, physical exertion	Lim et al. (2008)
accelerometer	motion disorders, fitness tracking	Lorenzi et al. (2016)

enabled parallel readout from glucose or lactate sensors. As biosensors are sensitive to biofouling and wear and tear due to their prolonged use, repeated sensing with multielectrodes increases the precision of the biochemical sensors by averaging the biosensor responses from electrode arrays. In a similar manner, Hong et al. demonstrated a fully integrated wireless system for the estimation of post-exercise blood glucose levels from sweat glucose levels (Fig. 9b) (Hong et al., 2018). The wrist-worn wearable system included a disposable patch with glucose and temperature sensors as well as an optical interface and an accelerometer for heart rate, SpO_2, and calculation of burned calories. The glucose sensors utilized three working electrodes that were operated sequentially via a multiplexer and a potentiostat for the detection of sweat glucose. The optical AFE utilized an integrated IC with three LEDs and a photodiode for heart rate and SpO_2 calculation from PPG signals. The accelerometer data (*i.e.,* burned calories), pre-exercise glucose levels, and sweat-to-blood correlation factors of each subject were used in the calculation of post-exercise glucose levels. Longitudinal measurement with the biochemical and physical sensors provided a stream of physiological data under dynamic and static exercise conditions, enabled correlation between human activity and blood glucose levels, and helped to estimate post-exercise blood glucose levels.

Fully integrated wearable systems with novel integration schemes and self-powered operation have also recently reported to minimize motion-induced noises and to enable battery-free operation (Yu et al., 2020; Zhao et al., 2020b). Fig. 9c demonstrates a wearable freestanding system for measurement of glucose, lactate, choline, and acceleration (Zhao et al., 2020b). The system comprises an optional iontophoresis module, a multilayer stack for fluid management, analyte sensing and transduction modules, and data acquisition and transmission with a total power consumption about 100 mW. Due to its unique out-of-plane design, the wearable system minimized strain accumulation on the signal pathway and revealed noise-free detection of amperometric

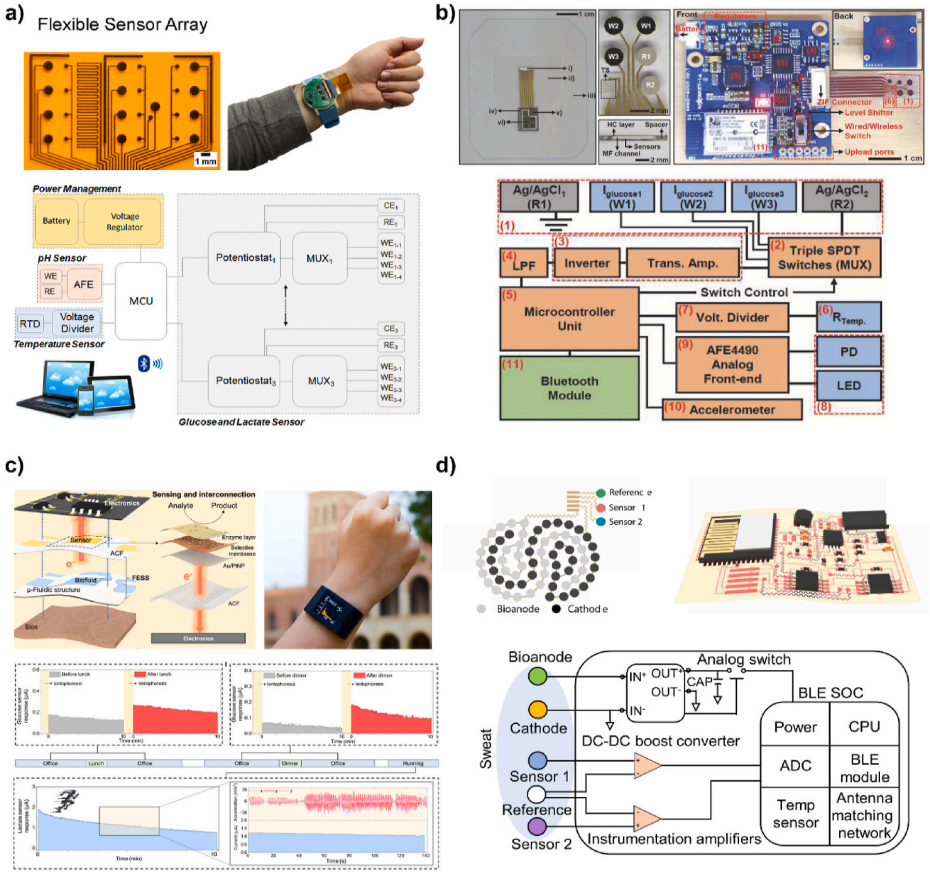

Fig. 9. Examples of wearable and wireless systems illustrating the integration of biochemical and biophysical sensors on a single platform. a) A wearable multiplexed biosensor system with a flexible sensing array for glucose, lactate, pH, and skin temperature measurement. Reproduced with permission (Yokus et al., 2020b). Copyright 2020, Elsevier. b) A disposable strip with a wrist-worn system for measurement of glucose, temperature, heart rate, SpO_2, and activity. Reproduced with permission (Hong et al., 2018). Copyright 2018, WILEY-VCH Verlag GmbH & Co. c) A freestanding electrochemical system with an out-of-plane signal interconnection design for strain isolation in the signal pathway. Reproduced with permission (Zhao et al., 2020b). Copyright 2020, Creative Commons Attribution 4.0 International License. d) A perspiration-powered soft electronic skin for urea, NH_4^+, glucose, pH, and temperature measurement. Reproduced with permission (Yu et al., 2020). Copyright 2020, The American Association for the Advancement of Science.

signals under exercise conditions. The study tested the robustness of the system to motion-induced noises by simultaneously recording biosensor and acceleration data while the subjects were engaging in various motions, such as punching, arm swinging, and forearm twisting. In a similar manner, Gao's research group created a biofuel-powered wearable multiplexed system for monitoring of urea, ammonia, glucose, pH, and skin temperature (Yu et al., 2020). The wearable system consisted of a biofuel cell (BFC), a boost converter, a biosensor array, signal conditioning circuitries, a system on chip with an integrated microcontroller, a BLE module, and a temperature sensor with an overall power consumption of 9.35 mW. The BFC relied on the presence of lactate in sweat and generated power as high as 3.6 mW cm^{-2}. The boost converter drew current from the BFCs, which was used for powering the rest of the circuitry. The study demonstrated self-powered operation and detection of urea and NH_4^+ or glucose and pH in sweat during an active exercise protocol.

Multimodal systems with different functionalities have been developed towards increasing the precision and robustness of the wearable systems to external factors (*e.g.*, sensor failure and motion-induced interferences), multisensory data correlation, self-powered operation, and prediction of post-exercise biomarker levels. Yet, there are still significant tradeoffs that need to be made when developing such wearable, wireless systems for longitudinal monitoring, such as power availability from self-powered devices and optimization of power consumption of the multisensory systems with iontophoretic sweat stimulation and wireless transmission.

5. Summary and future outlook

Wearable biochemical sensing from sweat, combined with biophysical sensing, and advanced analytics, offers new alternatives for noninvasive and real-time health monitoring, and it holds significant potential for identifying new longitudinal biomarkers. In this review, we outlined sweat sampling and collection methods that are important for achieving wearable health monitoring. We highlighted many skin-interfaced wearable sensors and systems for monitoring key sweat analytes and biophysical signals, such as metabolites, pH, electrolytes, heart rate, arterial oxygenation, sweat rate, and skin temperature, with an emphasis on their sensing techniques, system-level specifications, and multimodal functionalities. In our assessment of these technologies, there are still major outstanding challenges that restrict the broader acceptance, clinical implementation, and market adoption of such systems, but with each challenge comes the opportunities for novel developments.

From the technical perspective, there is still: (1) a lack of sweat-blood correlated data to support the popular sensing systems for glucose, lactate, and electrolytes. While sweat-blood correlations have been described for ethanol and cortisol in sweat (Buono 1999; Jia et al., 2016), recent reviews on sweat physiology have pointed towards the needed efforts to identify better correlated analytes (Heikenfeld et al., 2019). (2) The high variability and poor operational longevity of electrochemical sensors limit their standalone and longitudinal use; thus, (3) there is still a need to demonstrate the collection of high-density data streams for advanced analytics. From the applications perspective, user/clinician acceptance and deployment will require (1) identification of clinically-relevant value-added metrics, (2) robust implementation of fault-tolerant hardware, and (3) improved ease-of-use and wearability. Our perspectives on these cross-cutting challenges and potential multidisciplinary research areas are briefly outlined below:

Longitudinal sweat analysis for sedentary subjects, intra- and interpersonal sweat volume variance, and limited utility of sweat sensing. Current biochemical sensors rely on exercise, thermal, or iontophoretically induced sweat for sweat analysis, limiting its use only to ambulatory subjects and leaving out the sedentary and elderly population. Novel sweat extraction, storage, and sensing techniques need to be further explored for passive and power-free extraction of sweat to overcome challenges related to sweat generation or irritation due to the application of iontophoretic current to the skin. Ultimately, the next-generation of wearable health monitoring will require the capability of on-demand iontophoretic sweat induction, osmotic sweat pumping, or passive microfluidic collection across the varying excretion rates and intervals. To extend the utility of the sweat collection devices, operational lifting and waste collection systems must be developed.

Furthermore, researchers must use the emerging sweat collection devices and sweat rate sensors to collect and analyze sweat across a broader population and under varied operational conditions. Generating a *"sweat-ome"*, which compiles chemical and physical characteristics of sweat collected by different methods, will enable a more fundamental understanding of any sweat-blood correlations, and the collected pool of data will enable the use of more advanced analytical techniques, *e.g.,* machine learning and artificial intelligence, to improve the accuracy of sweat analyte measurements by compensating for the effect of intra- and interpersonal variation, analyte dilution, and equilibrium partitioning (Nyein et al., 2019; Yuan et al., 2019), while building confidence for clinically-valuable conclusions and defining both the fundamental and application limitations of sweat sensing.

Sensitive, stable, and extended sensor operation in the presence of common interferences. Current wearable biochemical and biophysical sensors have exhibited excellent performance *in vitro* or in narrowly-constrained human trials. Regarding wearable biochemical sensing, high sensitivity, dynamic range, linearity, and signal-to-noise ratio are desirable for the measurement of low levels of analytes in sweat or any target matrix with custom miniaturized electronic systems, so the continued development of novel biorecognition strategies, designing systems with redundant sensor arrays, or real-time calibration may lead to such improved metrics and extended operation in the laboratory. With that said, conventional clinical trials using non-invasive wearables for biochemical sensing with a corresponding intervention have not been reported. When systems are ready, extended, and repetitive human trials need to be carried out in the presence of external interferences, such as user error, motion artifacts, mechanical perturbations, ambient light, humidity, and temperature variation, to assess their operational stability for un-constrained daily use.

While many technical challenges must be overcome to deploy wearable systems in clinical trials, there is a contextual challenge that researchers must also overcome when designing and developing these wearable systems. It is important for researchers to better define their operational use-case. As many wearable systems are claimed to provide "continuous" sensing, this term is neither accurate nor necessary. The most common enzymatic electrochemical sensors drift and degrade with continuous operation, and the data density, as defined by the term "continuous", is modality and use-case dependent. A continuous optical heart rate sensor supposes a measurement frequency of 100–1000 Hz or higher; whereas a continuous glucose monitor's data is sufficiently relevant at minutes or even longer timescale. Accordingly, expectations and characterization of electrochemical sensor operations should better align with clinical relevance and more appropriately report their duration of utility. Most electrochemical sensors will accurately operate for minutes to hours at best, and demonstration of constant recording for minutes holds little clinical relevance. If appropriately duty-cycled and calibrated, a single sensor may provide days of information, and this information is much more valuable in integrating and implementing a multiplexed system. For example, a wearable system for monitoring of medication adherence may only require a daily measurement but operation for weeks, months, or longer. Therefore, demonstration of "longitudinal sensing" versus "continuous sensing" may be considered a more relevant term to use and target for researchers to aim their sensor development efforts.

Powering of wearable systems, low-power operation, and wireless communication. The increase in the number of sensing modalities in wearable systems warrant alternative power sources, wireless communication technologies, and efficient system-level operation for extended

operation. Most of the current wearable systems use lithium-based batteries, but they are rigid and difficult to miniaturize due to their energy density limitations. Alternative energy storage devices with high energy density, capacitance retention, leakage, and cycling performance and energy harvesting techniques (photovoltaic, thermoelectric, piezoelectric, triboelectric, and biofuel cells) should be employed to enable autonomous self-powering of wearable systems (Jung et al., 2015; Ostfeld et al., 2016; Zhao et al., 2019). Besides energy harvesting alternatives, the power consumption of the systems can be minimized by implementing system-level optimizations, such as selection of low-power nano-enabled sensors, low power radios, duty cycling, as well as the use of energy-efficient adaptive sampling and context-aware dynamic sensor selection techniques without sacrificing the accuracy of the physiological sensors (Dieffenderfer et al., 2016; Misra et al., 2019; Starliper et al., 2019).

Multimodal sensing and data mining. Fusion of biochemical and biophysical data in a wearable system for providing clinical diagnosis and treatment requires multimodal data fusion techniques with the objective of improving the signal quality and reliability, as well as reducing the uncertainty in data-based clinical decisions. Different pre-processing (data synchronization, filtering, feature extraction, normalization), data correlation, multiple hypothesis tests, and machine learning algorithms can be incorporated into the signal, feature, or decision-level data fusion for discovering the disease patterns, establishing the causes of potential pathologies, and administering a viable treatment (King et al., 2017; Lee et al., 2016).

Wearability, user acceptance, and scalability. As the wearable systems get more complicated with the addition of various sensing modalities, significant attention should be placed on biocompatibility, breathability, miniaturization, and overall mechanical reliability of the wearable devices to achieve aesthetically pleasing options that are robust against motion artifacts and device failures. Besides, cost-effective, and scalable fabrication methods should be implemented for large are coverage and commercial adoption of the new technologies.

Declaration of competing interest

The authors declare that they have no known competing financial interests or personal relationships that could have appeared to influence the work reported in this paper.

Acknowledgments

This work was supported by the National Science Foundation (EEC1160483) through an NSF Nanosystems Engineering Research Center (NERC) for Advanced Self-Powered Systems of Integrated Sensors and Technologies (ASSIST).

References

Agarwal, R.L., Kumar, D., Gurpreet Agarwal, D.K., Chabra, G.S., 2008. Diagnostic values of electrocardiogram in chronic obstructive pulmonary disease (Copd). Lung India 25 (2), 78–81.
Alizadeh, A., Burns, A., Lenigk, R., Gettings, R., Ashe, J., Porter, A., McCaul, M., Barrett, R., Diamond, D., White, P., Skeath, P., Tomczak, M., 2018. A wearable patch for continuous monitoring of sweat electrolytes during exertion. Lab Chip 18 (17), 2632–2641.
Allen, J., 2007. Photoplethysmography and its application in clinical physiological measurement. Physiol. Meas. 28 (3), R1–R39.
Anastasova, S., Crewther, B., Bembnowicz, P., Curto, V., Ip, H.M.D., Rosa, B., Yang, G.-Z., 2017. A wearable multisensing patch for continuous sweat monitoring. Biosens. Bioelectron. 93, 139–145.
Aoi, W., Marunaka, Y., 2014. Importance of pH homeostasis in metabolic health and diseases: crucial role of membrane proton transport. BioMed Res. Int., E598986
Apple, 2020. Activity Trackers.
Atkins, J.L., Butler, P.E.M., 2002. Hyperhidrosis: a review of current management. Plast. Reconstr. Surg. 110 (1), 222–228.
Baker, L.B., 2019. Physiology of sweat gland function: the roles of sweating and sweat composition in human health. Temperature (Austin, Tex.) 6 (3), 211–259.
Baker, L.B., Barnes, K.A., Anderson, M.L., Passe, D.H., Stofan, J.R., 2016. Normative data for regional sweat sodium concentration and whole-body sweating rate in athletes. J. Sports Sci. 34 (4), 358–368.
Baker, L.B., Stofan, J.R., Hamilton, A.A., Horswill, C.A., 2009. Comparison of regional patch collection vs. whole body washdown for measuring sweat sodium and potassium loss during exercise. J. Appl. Physiol. 107 (3), 887–895.
Bandodkar, A.J., Choi, J., Lee, S.P., Jeang, W.J., Agyare, P., Gutruf, P., Wang, S.Q., Sponenburg, R.A., Reeder, J.T., Schon, S., Ray, T.R., Chen, S.L., Mehta, S., Ruiz, S., Rogers, J.A., 2019a. Soft, skin-interfaced microfluidic systems with passive Galvanic stopwatches for precise chronometric sampling of sweat. Adv. Mater. 31 (32).
Bandodkar, A.J., Gutruf, P., Choi, J., Lee, K., Sekine, Y., Reeder, J.T., Jeang, W.J., Aranyosi, A.J., Lee, S.P., Model, J.B., Ghaffari, R., Su, C.J., Leshock, J.P., Ray, T., Verrillo, A., Thomas, K., Krishnamurthi, V., Han, S., Kim, J., Krishnan, S., Hang, T., Rogers, J.A., 2019b. Battery-free, skin-interfaced microfluidic/electronic systems for simultaneous electrochemical, colorimetric, and volumetric analysis of sweat. Sci. Adv. 5 (1), eaav3294.
Bandodkar, A.J., Jeang, W.J., Ghaffari, R., Rogers, J.A., 2019c. Wearable sensors for biochemical sweat analysis. Annu. Rev. Anal. Chem. 12 12, 1–22.
Bandodkar, A.J., Jeerapan, I., Wang, J., 2016. Wearable chemical sensors: present challenges and future prospects. ACS Sens. 1 (5), 464–482.
Bandodkar, A.J., Jia, W.Z., Yardimci, C., Wang, X., Ramirez, J., Wang, J., 2015. Tattoo-based noninvasive glucose monitoring: a proof-of-concept study. Anal. Chem. 87 (1), 394–398.
Bariya, M., Nyein, H.Y.Y., Javey, A., 2018a. Wearable sweat sensors. Nat. Electron. 1 (3), 160–171.
Bariya, M., Shahpar, Z., Park, H., Sun, J.F., Jung, Y., Gao, W., Nyein, H.Y.Y., Liaw, T.S., Tai, L.C., Ngo, Q.P., Chao, M.H., Zhao, Y.B., Hettick, M., Cho, G., Javey, A., 2018b. Roll-to-Roll gravure printed electrochemical sensors for wearable and medical devices. ACS Nano 12 (7), 6978–6987.
Benchirouf, A., Palaniyappan, S., Ramalingame, R., Raghunandan, P., Jagemann, T., Muller, C., Hietschold, M., Kanoun, O., 2016. Electrical properties of multi-walled carbon nanotubes/PEDOT:PSS nanocomposites thin films under temperature and humidity effects. Sensor. Actuator. B Chem. 224, 344–350.
Berger, D., 1999. A brief history of medical diagnosis and the birth of the clinical laboratory. Part 1–Ancient times through the 19th century. MLO: Med. Lab. Obs. 31 (7), 28–30, 32, 34-40.
Bowes, W.A., Corke, B.C., Hulka, J., 1989. Pulse oximetry - a review of the theory, accuracy, and clinical-applications. Obstet. Gynecol. 74 (3), 541–546.
Brake, D.J., Bates, G.P., 2003. Fluid losses and hydration status of industrial workers under thermal stress working extended shifts. Occup. Environ. Med. 60 (2), 90–96.
Brueck, A., Iftekhar, T., Stannard, A.B., Yelamarthi, K., Kaya, T., 2018. A real-time wireless sweat rate measurement system for physical activity monitoring. Sensors 18 (2).
Buono, M.J., 1999. Sweat ethanol concentrations are highly correlated with co-existing blood values in humans. Exp. Physiol. 84 (2), 401–404.
Campbell, A.S., Kim, J., Wang, J., 2018. Wearable electrochemical alcohol biosensors. Curr. Opin. Electrochem. 10, 126–135.
Casa, D.J., Armstrong, L.E., Hillman, S.K., Montain, S.J., Reiff, R.V., Rich, B.S.E., Roberts, W.O., Stone, J.A., 2000. National athletic trainers' association position statement: fluid replacement for athletes. J. Athl. Train. 35 (2), 212–224.
Cheuvront, S.N., Kenefick, R.W., 2014. Dehydration: physiology, assessment, and performance effects. Comp. Physiol. 4 (1), 257–285.
Choe, A., Yeom, J., Shanker, R., Kim, M.P., Kang, S., Ko, H., 2018. Stretchable and wearable colorimetric patches based on thermoresponsive plasmonic microgels embedded in a hydrogel film. NPG Asia Mater. 10, 912–922.
Choi, J., Bandodkar, A.J., Reeder, J.T., Ray, T.R., Turnquist, A., Kim, S.B., Nyberg, N., Hourlier-Fargette, A., Model, J.B., Aranyosi, A.J., Xu, S., Ghaffari, R., Rogers, J.A., 2019. Soft, skin-integrated multifunctional microfluidic systems for accurate colorimetric analysis of sweat biomarkers and temperature. ACS Sens. 4 (2), 379–388.
Choi, J., Kang, D., Han, S., Kim, S.B., Rogers, J.A., 2017a. Thin, soft, skin-mounted microfluidic networks with capillary bursting valves for chrono-sampling of sweat. Adv. Healthc. Mater. 6 (5).
Choi, J., Xue, Y.G., Xia, W., Ray, T.R., Reeder, J.T., Bandodkar, A.J., Kang, D., Xu, S., Huang, Y.G., Rogers, J.A., 2017b. Soft, skin-mounted microfluidic systems for measuring secretory fluidic pressures generated at the surface of the skin by eccrine sweat glands. Lab Chip 17 (15), 2572–2580.
Chung, H.U., Rwei, A.Y., Hourlier-Fargette, A., Xu, S., Lee, K., Dunne, E.C., Xie, Z., Liu, C., Carlini, A., Kim, D.H., Ryu, D., Kulikova, E., Cao, J., Odland, I.C., Fields, K.B., Hopkins, B., Banks, A., Ogle, C., Grande, D., Park, J.B., Kim, J., Irie, M., Jang, H., Lee, J., Park, Y., Kim, J., Jo, H.H., Hahm, H., Avila, R., Xu, Y., Namkoong, M., Kwak, J.W., Suen, E., Paulus, M.A., Kim, R.J., Parsons, B.V., Human, K.A., Kim, S.S., Patel, M., Reuther, W., Kim, H.S., Lee, S.H., Leedle, J.D., Yun, Y., Rigali, S., Son, T., Jung, I., Arafa, H., Soundararajan, V.R., Ollech, A., Shukla, A., Bradley, A., Schau, M., Rand, C.M., Marsillio, L.E., Harris, Z.L., Huang, Y., Hamvas, A., Paller, A. S., Weese-Mayer, D.E., Lee, J.Y., Rogers, J.A., 2020. Skin-interfaced biosensors for advanced wireless physiological monitoring in neonatal and pediatric intensive-care units. Nat. Med. 26 (3), 418–429.
Clark, R.P., 1984. Human skin temperature and its relevance in physiology and clinical assessment. In: Ring, E.F.J., Phillips, B. (Eds.), Recent Advances in Medical Thermology. Springer New York, Boston, MA, pp. 5–15.
Curto, V.F., Fay, C., Coyle, S., Byrne, R., O'Toole, C., Barry, C., Hughes, S., Moyna, N., Diamond, D., Benito-Lopez, F., 2012. Real-time sweat pH monitoring based on a wearable chemical barcode micro-fluidic platform incorporating ionic liquids. Sensor. Actuator. B Chem. 171, 1327–1334.

Derbyshire, P.J., Barr, H., Davis, F., Higson, S.P.J., 2012. Lactate in human sweat: a critical review of research to the present day. J. Physiol. Sci. 62 (6), 429–440.
Dieffenderfer, J., Goodell, H., Mills, S., McKnight, M., Yao, S.S., Lin, F.Y., Beppler, E., Bent, B., Lee, B., Misra, V., Zhu, Y., Oralkan, O., Strohmaier, J., Muth, J., Peden, D., Bozkurt, A., 2016. Low-power wearable systems for continuous monitoring of environment and health for chronic respiratory disease. Ieee J. Biomed. Health 20 (5).
Dill, D., Hall, F., Edwards, H., 1938. Changes in composition of sweat during acclimatization to heat. Am. J. Physiol. Leg. Content 123 (2), 412–419.
Elgendi, M., Fletcher, R., Liang, Y.B., Howard, N., Lovell, N.H., Abbott, D., Lim, K., Ward, R., 2019. The use of photoplethysmography for assessing hypertension. Npj Digit. Med. 2.
Emaminejad, S., Gao, W., Wu, E., Davies, Z.A., Nyein, H.Y.Y., Challa, S., Ryan, S.P., Fahad, H.M., Chen, K., Shahpar, Z., Talebi, S., Milla, C., Javey, A., Davis, R.W., 2017. Autonomous sweat extraction and analysis applied to cystic fibrosis and glucose monitoring using a fully integrated wearable platform. Proc. Natl. Acad. Sci. U.S.A. 114 (18), 4625–4630.
Fitbit, 2020.
Francis, J., Stamper, I., Heikenfeld, J., Gomez, E.F., 2019. Digital nanoliter to milliliter flow rate sensor with in vivo demonstration for continuous sweat rate measurement. Lab Chip 19 (1), 178–185.
Galli, A., Ambrosini, F., Lombardi, F., 2016. Holter monitoring and loop recorders: from research to clinical practice. Arrhythmia Electrophysiol. 5 (2), 136–143.
Gao, W., Emaminejad, S., Nyein, H.Y.Y., Challa, S., Chen, K., Peck, A., Fahad, H.M., Ota, H., Shiraki, H., Kiriya, D., Lien, D.-H., Brooks, G.A., Davis, R.W., Javey, A., 2016a. Fully integrated wearable sensor arrays for multiplexed in situ perspiration analysis. Nature 529 (7587), 509–514.
Gao, W., Nyein, H.Y.Y., Shahpar, Z., Fahad, H.M., Chen, K., Emaminejad, S., Gao, Y.J., Tai, L.C., Ota, H., Wu, E., Bullock, J., Zeng, Y.P., Lien, D.H., Javey, A., 2016b. Wearable microsensor array for multiplexed heavy metal monitoring of body fluids. ACS Sens. 1 (7), 866–874.
Garcia-Cordero, E., Bellando, F., Zhang, J.R., Wildhaber, F., Longo, J., Guerin, H., Ionescu, A.M., 2018a. Three-dimensional integrated ultra-low-volume passive microfluidics with ion-sensitive field-effect transistors for multiparameter wearable sweat analyzers. ACS Nano 12 (12), 12646–12656.
Garcia-Cordero, E., Wildhaber, F., Bellando, F., Longo, J., Fernandez-Bolanos, M., Guerin, H., Ionescu, A.M., 2018b. Embedded Passive Nano-Liter Micropump for Sweat Collection and Analysis. 2018 Ieee Micro Electro Mechanical Systems (Mems), pp. 1217–1220.
Gemperle, F., Kasabach, C., Stivoric, J., Bauer, M., Martin, R., 1998. Design for wearability. In: Second International Symposium on Wearable Computers - Digest of Papers, pp. 116–122.
Gibson, L.E., Cooke, R.E., 1959. A test for concentration of electrolytes in sweat in cystic fibrosis of the pancreas utilizing pilocarpine by iontophoresis. Pediatrics 23 (3), 545–549.
Glennon, T., O'Quigley, C., McCaul, M., Matzeu, G., Beirne, S., Wallace, G.G., Stroiescu, F., O'Mahoney, N., White, P., Diamond, D., 2016. SWEATCH': a wearable platform for harvesting and analysing sweat sodium content. Electroanalysis 28 (6), 1283–1289.
GlucoTrack, 2020. Noninvasive Glucose Monitoring.
Gopinathan, P.M., Pichan, G., Sharma, V.M., 1988. Role of dehydration in heat stress-induced variations in mental performance. Arch. Environ. Health 43 (1), 15–17.
Guk, K., Han, G., Lim, J., Jeong, K., Kang, T., Lim, E.K., Jung, J., 2019. Evolution of wearable devices with real-time disease monitoring for personalized healthcare. Nanomaterials (Basel) 9 (6).
Han, D., Khan, Y., Ting, J., Zhu, J., Combe, C., Wadsworth, A., McCulloch, I., Arias, A.C., 2020. Pulse oximetry using organic optoelectronics under ambient light. Adv. Mater. Technol. (U.S.A.) 5 (5), 1901122.
Han, S., Kim, J., Won, S.M., Ma, Y.J., Kang, D., Xie, Z.Q., Lee, K.T., Chung, H.U., Banks, A., Min, S., Heo, S.Y., Davies, C.R., Lee, J.W., Lee, C.H., Kim, B.H., Li, K., Zhou, Y.D., Wei, C., Feng, X., Huang, Y.G., Rogers, J.A., 2018. Battery-free, wireless sensors for full-body pressure and temperature mapping. Sci. Transl. Med. 10 (435).
Han, W., He, H., Zhang, L., Dong, C., Zeng, H., Dai, Y., Xing, L., Zhang, Y., Xue, X., 2017. A self-powered wearable noninvasive electronic-skin for perspiration analysis based on piezo-biosensing unit matrix of enzyme/ZnO nanoarrays. ACS Appl. Mater. Interfaces 9 (35), 29526–29537.
Hauke, A., Simmers, P., Ojha, Y.R., Cameron, B.D., Ballweg, R., Zhang, T., Twine, N., Brothers, M., Gomez, E., Heikenfeld, J., 2018a. Complete validation of a continuous and blood-correlated sweat biosensing device with integrated sweat stimulation. Lab Chip 18 (24), 3750–3759.
Hauke, A., Simmers, P., Ojha, Y.R., Cameron, B.D., Ballweg, R., Zhang, T., Twine, N., Brothers, M., Gomez, E., Heikenfeld, J., 2018b. Complete validation of a continuous and blood-correlated sweat biosensing device with integrated sweat stimulation. Lab Chip 18 (24).
Haveman, M.E., Kleiss, S.F., Ma, K.F., Vos, C.G., Unlu, C., Schuurmann, R.C.L., Bokkers, R.P.H., Hermens, H.J., De Vries, J.P.P.M., 2019. Telemedicine in patients with peripheral arterial disease: is it worth the effort? Expet Rev. Med. Dev. 16 (9), 1–10.
He, X.C., Xu, T.L., Gu, Z., Gao, W., Xu, L.P., Pan, T.R., Zhang, X.J., 2019. Flexible and superwettable bands as a platform toward sweat sampling and sensing. Anal. Chem. 91 (7), 4296–4300.
Heikenfeld, J., 2016. Non-invasive analyte access and sensing through eccrine sweat: challenges and outlook circa 2016. Electroanalysis 28 (6), 1242–1249.
Heikenfeld, J., Jajack, A., Feldman, B., Granger, S.W., Gaitonde, S., Begtrup, G., Katchman, B.A., 2019. Accessing analytes in biofluids for peripheral biochemical monitoring. Nat. Biotechnol. 37 (4), 407–419.
Heikenfeld, J., Jajack, A., Rogers, J., Gutruf, P., Tian, L., Pan, T., Li, R., Khine, M., Kim, J., Wang, J., Kim, J., 2017. Wearable sensors: modalities, challenges, and prospects. Lab Chip 18 (2), 217–248.
Hexoskin, 2020. Heart Rate and Respiratory Rate Monitoring.
Hong, Y.J., Lee, H., Kim, J., Lee, M., Choi, H.J., Hyeon, T., Kim, D.H., 2018. Multifunctional wearable system that integrates sweat-based sensing and vital-sign monitoring to estimate pre-/post-exercise glucose levels. Adv. Funct. Mater. 28 (47).
Hovorka, R., 2006. Continuous glucose monitoring and closed-loop systems. Diabet. Med. 23 (1), 1–12.
Huang, X., Liu, Y.H., Chen, K.L., Shin, W.J., Lu, C.J., Kong, G.W., Patnaik, D., Lee, S.H., Cortes, J.F., Rogers, J.A., 2014. Stretchable, wireless sensors and functional substrates for epidermal characterization of sweat. Small 10 (15), 3083–3090.
iHealth, 2020a. Wireless Activity and Sleep Tracker.
iHealth, 2020b. Wireless Wrist Blood Pressure Monitor.
Imani, S., Bandodkar, A.J., Mohan, A.M.V., Kumar, R., Yu, S.F., Wang, J., Mercier, P.P., 2016a. A wearable chemical-electrophysiological hybrid biosensing system for real-time health and fitness monitoring. Nat. Commun. 7.
Imani, S., Mercier, P.P., Bandodkar, A.J., Kim, J., Wang, J., 2016b. Wearable chemical sensors: opportunities and challenges. In: 2016 Ieee International Symposium on Circuits and Systems (Iscas), pp. 1122–1125.
Jeerapan, I., Sempionatto, J.R., Pavinatto, A., You, J.M., Wang, J., 2016. Stretchable biofuel cells as wearable textile-based self-powered sensors. J. Mater. Chem. 4 (47), 18342–18353.
Jia, M., Chew, W.M., Feinstein, Y., Skeath, P., Sternberg, E.M., 2016. Quantification of cortisol in human eccrine sweat by liquid chromatography - tandem mass spectrometry. Analyst 141 (6), 2053–2060.
Jia, W., Bandodkar, A.J., Valdés-Ramírez, G., Windmiller, J.R., Yang, Z., Ramírez, J., Chan, G., Wang, J., 2013. Electrochemical tattoo biosensors for real-time noninvasive lactate monitoring in human perspiration. Anal. Chem. 85 (14), 6553–6560.
Jung, S., Hong, S., Kim, J., Lee, S., Hyeon, T., Lee, M., Kim, D.H., 2015. Wearable fall detector using integrated sensors and energy devices. Sci. Rep. (U.K.) 5.
Kamal, A.A.R., Harness, J.B., Irving, G., Mearns, A.J., 1989. Skin photoplethysmography - a review. Comput. Methods Progr. Biomed. 28 (4), 257–269.
Kassal, P., Zubak, M., Scheipl, G., Mohr, G.J., Steinberg, M.D., Steinberg, I.M., 2017. Smart bandage with wireless connectivity for optical monitoring of pH. Sensor. Actuator. B Chem. 246, 455–460.
Kelechi, T.J., Michel, Y., 2007. A descriptive study of skin temperature, tissue perfusion, and tissue oxygen in patients with chronic venous disease. Biol. Res. Nurs. 9 (1), 70–80.
Kelly, G., 2006. Body temperature variability (Part 1): a review of the history of body temperature and its variability due to site selection, biological rhythms, fitness, and aging. Alternative Med. Rev. 11 (4), 278–293.
Kelly, G.S., 2007. Body temperature variability (part 2): masking influences of body temperature variability and a review of body temperature variability in disease. Alternative Med. Rev. 12 (1), 49–62.
Khan, Y., Garg, M., Gui, Q., Schadt, M., Gaikwad, A., Han, D.G., Yamamoto, N.A.D., Hart, P., Welte, R., Wilson, W., Czarnecki, S., Poliks, M., Jin, Z.P., Ghose, K., Egitto, F., Turner, J., Arias, A.C., 2016. Flexible hybrid electronics: direct interfacing of soft and hard electronics for wearable health monitoring. Adv. Funct. Mater. 26 (47), 8764–8775.
Khan, Y., Han, D., Pierre, A., Ting, J., Wang, X.C., Lochner, C.M., Bovo, G., Yaacobi-Gross, N., Newsome, C., Wilson, R., Arias, A.C., 2018. A flexible organic reflectance oximeter array. Proc. Natl. Acad. Sci. U.S.A. 115 (47), E11015–E11024.
Kim, J., Campbell, A.S., de Avila, B.E.F., Wang, J., 2019. Wearable biosensors for healthcare monitoring. Nat. Biotechnol. 37 (4), 389–406.
Kim, J., Salvatore, G.A., Araki, H., Chiarelli, A.M., Xie, Z., Banks, A., Sheng, X., Liu, Y., Lee, J.W., Jang, K.-I., Heo, S.Y., Cho, K., Luo, H., Zimmerman, B., Kim, J., Yan, L., Feng, X., Xu, S., Fabiani, M., Gratton, G., Huang, Y., Paik, U., Rogers, J.A., 2016. Battery-free, stretchable optoelectronic systems for wireless optical characterization of the skin. Sci. Adv. 2 (8).
Kim, S.B., Lee, K., Raj, M.S., Lee, B., Reeder, J.T., Koo, J., Hourlier-Fargette, A., Bandodkar, A.J., Won, S.M., Sekine, Y., Choi, J., Zhang, Y., Yoon, J., Kim, B.H., Yun, Y., Lee, S., Shin, J., Kim, J., Ghaffari, R., Rogers, J.A., 2018a. Soft, skin-interfaced microfluidic systems with wireless, battery-free electronics for digital, real-time tracking of sweat loss and electrolyte composition. Small 14 (45).
Kim, S.B., Zhang, Y., Won, S.M., Bandodkar, A.J., Sekine, Y., Xue, Y., Koo, J., Harshman, S.W., Martin, J.A., Park, J.M., Ray, T.R., Crawford, K.E., Lee, K.T., Choi, J., Pitsch, R.L., Grigsby, C.C., Strang, A.J., Chen, Y.Y., Xu, S., Kim, J., Koh, A., Ha, J.S., Huang, Y., Kim, S.W., Rogers, J.A., 2018b. Super-absorbent polymer valves and colorimetric chemistries for time-sequenced discrete sampling and chloride analysis of sweat via skin-mounted soft microfluidics. Small 14 (12).
King, R.C., Villeneuve, E., White, R.J., Sherratt, R.S., Holderbaum, W., Harwin, W.S., 2017. Application of data fusion techniques and technologies for wearable health monitoring. Med. Eng. Phys. 42, 1–12.
Kintz, P., Tracqui, A., Mangin, P., Edel, Y., 1996. Sweat testing in opioid users with a sweat patch. J. Anal. Toxicol. 20 (6), 393–397.
Koh, A., Kang, D., Xue, Y., Lee, S., Pielak, R.M., Kim, J., Hwang, T., Min, S., Banks, A., Bastien, P., Manco, M.C., Wang, L., Ammann, K.R., Jang, K.I., Won, P., Han, S., Ghaffari, R., Paik, U., Slepian, M.J., Balooch, G., Huang, Y.G., Rogers, J.A., 2016. A soft, wearable microfluidic device for the capture, storage, and colorimetric sensing of sweat. Sci. Transl. Med. 8 (366).
Kreisberg, R.A., 1984. Pathogenesis and management of lactic-acidosis. Annu. Rev. Med. 35, 181–193.
Krishnan, S.R., Su, C.J., Xie, Z.Q., Patel, M., Madhvapathy, S.R., Xu, Y.S., Freudman, J., Ng, B., Heo, S.Y., Wang, H.L., Ray, T.R., Leshock, J., Stankiewicz, I., Feng, X.,

Huang, Y.G., Gutruf, P., Rogers, J.A., 2018. Wireless, battery-free epidermal electronics for continuous, quantitative, multimodal thermal characterization of skin. Small 14 (47).
Kulkarni, P., Öztürk, Y., 2007. Requirements and design spaces of mobile medical care. Mob. Comput. Commun. Rev. 11, 12–30.
Kumar, L.S.S., Wang, X., Hagen, J., Naik, R., Papautsky, I., Heikenfeld, J., 2016. Label free nano-aptasensor for interleukin-6 in protein-dilute bio fluids such as sweat. Anal. Methods 8 (17), 3440–3444.
Lee, H., Choi, T.K., Lee, Y.B., Cho, H.R., Ghaffari, R., Wang, L., Choi, H.J., Chung, T.D., Lu, N., Hyeon, T., Choi, S.H., Kim, D.-H., 2016. A graphene-based electrochemical device with thermoresponsive microneedles for diabetes monitoring and therapy. Nat. Nanotechnol. 11 (6), 566–572.
Lee, H., Song, C., Hong, Y.S., Kim, M.S., Cho, H.R., Kang, T., Shin, K., Choi, S.H., Hyeon, T., Kim, D.H., 2017a. Wearable/disposable sweat-based glucose monitoring device with multistage transdermal drug delivery module. Sci. Adv. 3 (3).
Lee, Y.K., Jang, K.I., Ma, Y.J., Koh, A., Chen, H., Jung, H.N., Kim, Y., Kwak, J.W., Wang, L., Xue, Y.G., Yang, Y.Y., Tian, W.L., Jiang, Y., Zhang, Y.H., Feng, X., Huang, Y.G., Rogers, J.A., 2017b. Chemical sensing systems that utilize soft electronics on thin elastomeric substrates with open cellular designs. Adv. Funct. Mater. 27 (9).
Legner, C., Kalwa, U., Patel, V., Chesmore, A., Pandey, S., 2019. Sweat sensing in the smart wearables era: towards integrative, multifunctional and body-compliant perspiration analysis. Sensor Actuat a-Phys 296, 200–221.
Leithead, C., Lind, Ar, 1964. Heat-stress and heat disorders. Roy. Soc. Health J. 84 (4), 213-213.
Li, M., Wang, L., Liu, R., Li, J., Zhang, Q., Shi, G., Li, Y., Hou, C., Wang, H., 2021. A highly integrated sensing paper for wearable electrochemical sweat analysis. Biosens. Bioelectron. 174, 112828.
Lim, C.L., Byrne, C., Lee, J.K.W., 2008. Human thermoregulation and measurement of body temperature in exercise and clinical settings. Ann. Acad. Med. Singapore 37 (4), 347–353.
Lin, H.S., Zhao, Y.C., Lin, S.Y., Wang, B., Yeung, C., Cheng, X.B., Wang, Z.Q., Cai, T.Y., Yu, W.Z., King, K., Tan, J.W., Salahi, K., Hojaiji, H., Emaminejad, S., 2019. A rapid and low-cost fabrication and integration scheme to render 3D microfluidic architectures for wearable biofluid sampling, manipulation, and sensing. Lab Chip 19 (17), 2844–2853.
Lin, S.Y., Wang, B., Zhao, Y.C., Shih, R., Cheng, X.B., Yu, W.Z., Hojaiji, H., Lin, H.S., Hoffman, C., Ly, D., Tan, J.W., Chen, Y., Di Carlo, D., Milla, C., Emaminejad, S., 2020. Natural perspiration sampling and in situ electrochemical analysis with hydrogel micropatches for user-identifiable and wireless chemo/biosensing. ACS Sens. 5 (1), 93–102.
Liu, C.H., Xu, T.L., Wang, D.D., Zhang, X.J., 2020. The role of sampling in wearable sweat sensors. Talanta 212.
Liu, G., Hob, C., Slappey, N., Zhou, Z., Snelgrove, S.E., Brown, M., Grabinski, A., Guo, X., Chen, D.Y., Miller, K., Edwards, J., Kaya, T., 2016. A wearable conductivity sensor for wireless real-time sweat monitoring. Sensor. Actuator. B Chem. 227, 35–42.
Lorenzi, P., Rao, R., Romano, G., Kita, A., Irrera, F., 2016. Mobile devices for the real-time detection of specific human motion disorders. Ieee Sens. J. 16 (23), 8220–8227.
Lorincz, K., Malan, D.J., Fulford-Jones, T.R.F., Nawoj, A., Clavel, A., Shnayder, V., Mainland, G., Welsh, M., Moulton, S., 2004. Sensor networks for emergency response: challenges and opportunities. Ieee Pervas Comput. 3 (4), 16–23.
Lu, Y., Jiang, K., Chen, D., Shen, G.Z., 2019. Wearable sweat monitoring system with integrated micro-supercapacitors. Nano Energy 58, 624–632.
Martin, A., Kim, J., Kurniawan, J.F., Sempionatto, J.R., Moreto, J.R., Tang, G.D., Campbell, A.S., Shin, A., Lee, M.Y., Liu, X.F., Wang, J., 2017. Epidermal microfluidic electrochemical detection system: enhanced sweat sampling and metabolite detection. ACS Sens. 2 (12), 1860–1868.
Matzeu, G., Fay, C., Vaillant, A., Coyle, S., Diamond, D., 2016. A wearable device for monitoring sweat rates via image analysis. Ieee Trans. Bio-Med. Eng. 63 (8), 1672–1680.
Maughan, R.J., Shirreffs, S.M., 2010. Dehydration and rehydration in competitive sport. Scand. J. Med. Sci. Sports 20, 40–47.
Mergenthaler, P., Lindauer, U., Dienel, G.A., Meisel, A., 2013. Sugar for the brain: the role of glucose in physiological and pathological brain function. Trends Neurosci. 36 (10), 587–597.
Michahelles, F., Matter, P., Schmidt, A., Schiele, B., 2003. Applying wearable sensors to avalanche rescue. Comput. Graph (U.K.) 27 (6), 839–847.
Misra, V., Bozkurt, A., Calhoun, B.H., Datta, S., Dickey, M., Kiani, M., Lach, J., Lee, B., Jur, J., Oralkan, O., Ozturk, M., Rajagopalan, R., Roundy, S., Strohmaier, J., Trolier-McKinstry, S., Vashaee, D., Wentzloff, D., Werner, D., 2019. Optimizing the energy balance to achieve autonomous self-powering for vigilant health and IoT applications. J. Phys. Conf. 1407, 012001.
Moyer, J., Wilson, D., Finkelshtein, I., Wong, B., Potts, R., 2012. Correlation between sweat glucose and blood glucose in subjects with diabetes. Diabetes Technol. Therapeut. 14 (5), 398–402.
Nakata, S., Arie, T., Akita, S., Takei, K., 2017. Wearable, flexible, and multifunctional healthcare device with an ISFET chemical sensor for simultaneous sweat pH and skin temperature monitoring. ACS Sens. 2 (3), 443–448.
Nonin Medical, 2020. Pulse Oximeters.
Nyein, H.Y.Y., Bariya, M., Kivimaki, L., Uusitalo, S., Liaw, T.S., Jansson, E., Ahn, C.H., Hangasky, J.A., Zhao, J.Q., Lin, Y.J., Happonen, T., Chao, M.H., Liedert, C., Zhao, Y. B., Tai, L.C., Hiltunen, J., Javey, A., 2019. Regional and correlative sweat analysis using high-throughput microfluidic sensing patches toward decoding sweat. Sci. Adv. 5 (8).
Nyein, H.Y.Y., Tai, L.C., Ngo, Q.P., Chao, M., Zhang, G.B., Gao, W., Bariya, M., Bullock, J., Kim, H., Fahad, H.M., Javey, A., 2018a. A wearable microfluidic sensing patch for dynamic sweat secretion analysis. ACS Sens. 3 (5), 944–952.
Nyein, H.Y.Y., Tai, L.C., Ngo, Q.P., Chao, M.H., Zhang, G.B., Gao, W., Bariya, M., Bullock, J., Kim, H., Fahad, H.M., Javey, A., 2018b. A wearable microfluidic sensing patch for dynamic sweat secretion analysis. ACS Sens. 3 (5), 944–952.
Ostfeld, A.E., Gaikwad, A.M., Khan, Y., Arias, A.C., 2016. High-performance flexible energy storage and harvesting system for wearable electronics. Sci. Rep. (U.K.) 6.
Pal, A., Goswami, D., Cuellar, H.E., Castro, B., Kuang, S.H., Martinez, R.V., 2018. Early detection and monitoring of chronic wounds using low-cost, omniphobic paper-based smart bandages. Biosens. Bioelectron. 117, 696–705.
Pantelopoulos, A., Bourbakis, N., 2008. A survey on wearable biosensor systems for health monitoring. In: Conf Proc IEEE Eng Med Biol Soc 2008, pp. 4887–4890.
Parlak, O., Keene, S.T., Marais, A., Curto, V.F., Salleo, A., 2018. Molecularly selective nanoporous membrane-based wearable organic electrochemical device for noninvasive cortisol sensing. Sci. Adv. 4 (7).
Parrilla, M., Guinovart, T., Ferre, J., Blondeau, P., Andrade, F.J., 2019a. A wearable paper-based sweat sensor for human perspiration monitoring. Adv. Healthc. Mater. 8 (16), e1900342.
Parrilla, M., Guinovart, T., Ferre, J., Blondeau, P., Andrade, F.J., 2019b. A wearable paper-based sweat sensor for human perspiration monitoring. Advanced Healthcare Materials.
Patterson, M.J., Galloway, S.D.R., Nimmo, M.A., 2000. Variations in regional sweat composition in normal human males. Exp. Physiol. 85 (6), 869–875.
Pelaez, E.A., Villegas, E.R., 2007. LED power reduction trade-offs for ambulatory pulse oximetry. In: 2007 Annual International Conference of the Ieee Engineering in Medicine and Biology Society, Vols. 1–16, pp. 2296–2299.
Peng, R., Sonner, Z., Hauke, A., Wilder, E., Kasting, J., Gaillard, T., Swaille, D., Sherman, F., Mao, X., Hagen, J., Murdock, R., Heikenfeld, J., 2016. A new oil/membrane approach for integrated sweat sampling and sensing: sample volumes reduced from mu L's to nL's and reduction of analyte contamination from skin. Lab Chip 16 (22), 4415–4423.
Percival, S.L., McCarty, S., Hunt, J.A., Woods, E.J., 2014. The effects of pH on wound healing, biofilms, and antimicrobial efficacy. Wound Repair Regen. 22 (2), 174–186.
Rathee, K., Dhull, V., Dhull, R., Singh, S., 2016. Biosensors based on electrochemical lactate detection: a comprehensive review. Biochem. Biophys. Rep. 5, 35–54.
Ray, T.R., Choi, J., Bandodkar, A.J., Krishnan, S., Gutruf, P., Tian, L.M., Ghaffari, R., Rogers, J.A., 2019. Bio-integrated wearable systems: a comprehensive review. Chem. Rev. 119 (8), 5461–5533.
Reeder, J.T., Choi, J., Xue, Y.G., Gutruf, P., Hanson, J., Liu, M., Ray, T., Bandodkar, A.J., Avila, R., Xia, W., Krishnan, S., Xu, S., Barnes, K., Pahnke, M., Ghaffari, R., Huang, Y., Rogers, J.A., 2019. Waterproof, electronics-enabled, epidermal microfluidic devices for sweat collection, biomarker analysis, and thermography in aquatic settings. Sci. Adv. 5 (1).
Rhee, S., Yang, B.H., Asada, H.H., 2001. Artifact-resistant power-efficient design of finger-ring plethysmographic sensors. Ieee Trans. Bio-Med. Eng. 48 (7), 795–805.
Robinson, S., Robinson, A.H., 1954. Chemical composition of sweat. Physiol. Rev. 34 (2), 202–220.
Roederer, A., Weimer, J., DiMartino, J., Gutsche, J., Lee, I., 2015. Robust monitoring of hypovolemia in intensive care patients using photoplethysmogram signals. In: 2015 37th Annual International Conference of the Ieee Engineering in Medicine and Biology Society. Embc, pp. 1504–1507.
Rose, D.P., Ratterman, M.E., Griffin, D.K., Hou, L., Kelley-Loughnane, N., Naik, R.R., Hagen, J.A., Papautsky, I., Heikenfeld, J.C., 2015. Adhesive RFID sensor patch for monitoring of sweat electrolytes. Ieee Trans. Bio-Med. Eng. 62 (6), 1457–1465.
Saha, T., Fang, J., Mukherjee, S., Dickey, M.D., Velev, O.D., 2021. Wearable osmotic-capillary patch for prolonged sweat harvesting and sensing. ACS Appl. Mater. Interfaces 13 (7), 8071–8081.
Salvo, P., Pingitore, A., Barbini, A., Di Francesco, F., 2018. A wearable sweat rate sensor to monitor the athletes' performance during training. Sci. Sports 33 (2), e51–e58.
Samsung, 2020. Activity Trackers.
Sato, K., Sato, F., 1983. Individual variations in structure and function of human eccrine sweat gland. Am. J. Physiol. 245 (2), R203–R208.
Sekar, M., Pandiaraj, M., Bhansali, S., Ponpandian, N., Viswanathan, C., 2019. Carbon fiber based electrochemical sensor for sweat cortisol measurement. Sci. Rep. 9 (1), 403.
Sekine, Y., Kim, S.B., Zhang, Y., Bandodkar, A.J., Xu, S., Choi, J., Irie, M., Ray, T.R., Kohli, P., Kozai, N., Sugita, T., Wu, Y.X., Lee, K., Lee, K.T., Ghaffari, R., Rogers, J.A., 2018. A fluorometric skin-interfaced microfluidic device and smartphone imaging module for in situ quantitative analysis of sweat chemistry. Lab Chip 18 (15), 2178–2186.
Selvam, A.P., Muthukumar, S., Kamakoti, V., Prasad, S., 2016. A wearable biochemical sensor for monitoring alcohol consumption lifestyle through Ethyl glucuronide (EtG) detection in human sweat. Sci. Rep. (U.K.) 6.
Sempionatto, J.R., Jeerapan, I., Krishnan, S., Wang, J., 2020a. Wearable chemical sensors: emerging systems for on-body analytical chemistry. Anal. Chem. 92 (1), 378–396.
Sempionatto, J.R., Khorshed, A.A., Ahmed, A., De Loyola e Silva, A.N., Barfidokht, A., Yin, L., Goud, K.Y., Mohamed, M.A., Bailey, E., May, J., Aebischer, C., Chatelle, C., Wang, J., 2020b. Epidermal enzymatic biosensors for sweat vitamin C: toward personalized nutrition. ACS Sens. 5 (6), 1804–1813.
Sempionatto, J.R., Nakagawa, T., Pavinatto, A., Mensah, S.T., Imani, S., Mercier, P., Wang, J., 2017. Eyeglasses based wireless electrolyte and metabolite sensor platform. Lab Chip 17 (10), 1834–1842.
Sessa, F., Anna, V., Messina, G., Cibelli, G., Monda, V., Marsala, G., Ruberto, M., Biondi, A., Cascio, O., Bertozzi, G., Pisanelli, D., Maglietta, F., Messina, A.,

Mollica, M.P., Salerno, M., 2018. Heart rate variability as predictive factor for sudden cardiac death. Aging (U.S.A.) 10 (2), 166–177.
Shay, T., Saha, T., Dickey, M.D., Velev, O.D., 2020. Principles of long-term fluids handling in paper-based wearables with capillary–evaporative transport. Biomicrofluidics 14 (3), 034112.
Simmers, P., Li, S.K., Kasting, G., Heikenfeld, J., 2018. Prolonged and localized sweat stimulation by iontophoretic delivery of the slowly-metabolized cholinergic agent carbachol. J. Dermatol. Sci. 89 (1), 40–51.
Singh, M., Verma, N., Garg, A.K., Redhu, N., 2008. Urea biosensors. Sensor. Actuator. B Chem. 134 (1), 345–351.
Sonner, Z., Wilder, E., Heikenfeld, J., Kasting, G., Beyette, F., Swaile, D., Sherman, F., Joyce, J., Hagen, J., Kelley-Loughnane, N., Naik, R., 2015. The microfluidics of the eccrine sweat gland, including biomarker partitioning, transport, and biosensing implications. Biomicrofluidics 9 (3), 031301.
Starliper, N., Mohammadzadeh, F., Songkakul, T., Hernandez, M., Bozkurt, A., Lobaton, E., 2019. Activity-aware wearable system for power-efficient prediction of physiological responses. Sensors (Basel) 19 (3).
Tai, L.-C., Ahn, C.H., Nyein, H.Y.Y., Ji, W., Bariya, M., Lin, Y., Li, L., Javey, A., 2020. Nicotine monitoring with a wearable sweat band. ACS Sens. 5 (6), 1831–1837.
Tai, L.C., Gao, W., Chao, M.H., Bariya, M., Ngo, Q.P., Shahpar, Z., Nyein, H.Y.Y., Park, H., Sun, J., Jung, Y., Wu, E., Fahad, H.M., Lien, D.H., Ota, H., Cho, G., Javey, A., 2018. Methylxanthine drug monitoring with wearable sweat sensors. Adv. Mater. 30 (23).
Takei, K., Gao, W., Wang, C., Javey, A., 2019. Physical and chemical sensing with electronic skin. Proc. Ieee 107 (10), 2155–2167.
Tamura, T., 2019. Current progress of photoplethysmography and SPO2 for health monitoring. Biomed. Eng. Lett. 9 (1), 21–36.
Torrente-Rodriguez, R.M., Tu, J.B., Yang, Y.R., Min, J.H., Wang, M.Q., Song, Y., Yu, Y., Xu, C.H., Ye, C., IsHak, W.W., Gao, W., 2020. Investigation of cortisol dynamics in human sweat using a graphene-based wireless mHealth system. Matter 2 (4), 921–937.
Tricoli, A., Neri, G., 2018. Miniaturized bio-and chemical-sensors for point-of-care monitoring of chronic kidney diseases. Sensors 18 (4).
Twine, N.B., Norton, R.M., Brothers, M.C., Hauke, A., Gomez, E.F., Heikenfeld, J., 2018. Open nanofluidic films with rapid transport and no analyte exchange for ultra-low sample volumes. Lab Chip 18 (18), 2816–2825.
Vashist, S.K., 2012. Non-invasive glucose monitoring technology in diabetes management: a review. Anal. Chim. Acta 750, 16–27.
Wagner, P.D., 2008. The biology of oxygen. Eur. Respir. J. 31 (4), 887–890.
Wang, J., 2008. Electrochemical glucose biosensors. Chem. Rev. 108 (2), 814–825.
Wang, S.Q., Wu, Y.J., Gu, Y., Li, T., Luo, H., Li, L.H., Bai, Y.Y., Li, L.L., Liu, L., Cao, Y.D., Ding, H.Y., Zhang, T., 2017. Wearable sweatband sensor platform based on gold nanodendrite array as efficient solid contact of ion-selective electrode. Anal. Chem. 89 (19), 10224–10231.
Wang, Y.F., Sekine, T., Takeda, Y., Yokosawa, K., Matsui, H., Kumaki, D., Shiba, T., Nishikawa, T., Tokito, S., 2020. Fully printed PEDOT:PSS-based temperature sensor with high humidity stability for wireless healthcare monitoring. Sci. Rep. 10 (1), 2467.
Webster, J.G., 1997. Design of Pulse Oximeters. CRC Press.
Wiorek, A., Parrilla, M., Cuartero, M., Crespo, G.A., 2020. Epidermal patch with glucose biosensor: pH and temperature correction toward more accurate sweat analysis during sport practice. Anal. Chem. 92 (14), 10153–10161.
Xu, G., Cheng, C., Liu, Z., Yuan, W., Wu, X., Lu, Y., Low, S.S., Liu, J., Zhu, L., Ji, D., Li, S., Chen, Z., Wang, L., Yang, Q., Cui, Z., Liu, Q., 2019. Battery-free and wireless epidermal electrochemical system with all-printed stretchable electrode array for multiplexed in situ sweat analysis. Adv. Mater. Technol. (U.S.A.) 4 (7), 1800658.
Yamamoto, Y., Yamamoto, D., Takada, M., Naito, H., Arie, T., Akita, S., Takei, K., 2017. Efficient skin temperature sensor and stable gel-less sticky ECG sensor for a wearable flexible healthcare patch. Adv. Healthc. Mater. 6 (17).
Yang, Y.R., Song, Y., Bo, X.J., Min, J.H., Pak, O.S., Zhu, L.L., Wang, M.Q., Tu, J.B., Kogan, A., Zhang, H.X., Hsiai, T.K., Li, Z.P., Gao, W., 2020. A laser-engraved wearable sensor for sensitive detection of uric acid and tyrosine in sweat. Nat. Biotechnol. 38 (2), 217–224.
Yokota, T., Zalar, P., Kaltenbrunner, M., Jinno, H., Matsuhisa, N., Kitanosako, H., Tachibana, Y., Yukita, W., Koizumi, M., Someya, T., 2016. Ultraflexible organic photonic skin. Sci. Adv. 2 (4).
Yokus, M., Agcayazi, T., Traenkle, M., Bozkurt, A., Daniele, M.A., 2020a. Wearable sweat rate sensors. In: IEEE (Ed.), IEEE SENSORS 2020. IEEE, pp. 1–4.
Yokus, M.A., Songkakul, T., Pozdin, V.A., Bozkurt, A., Daniele, M.A., 2020b. Wearable multiplexed biosensor system toward continuous monitoring of metabolites. Biosens. Bioelectron. 153, 112038.
Yousef, Q., Reaz, M.B.I., Ali, M.A.M., 2012. The analysis of PPG morphology: investigating the effects of aging on arterial compliance. Meas. Sci. Rev. 12 (6), 266–271.
Yu, Y., Nassar, J., Xu, C., Min, J., Yang, Y., Dai, A., Doshi, R., Huang, A., Song, Y., Gehlhar, R., Ames, A.D., Gao, W., 2020. Biofuel-powered soft electronic skin with multiplexed and wireless sensing for human-machine interfaces. Sci. Robot. 5 (41), eaaz7946.
Yuan, Z., Hou, L., Bariya, M., Nyein, H.Y.Y., Tai, L.C., Ji, W.B., Liabc, L., Javey, A., 2019. A multi-modal sweat sensing patch for cross-verification of sweat rate, total ionic charge, and Na+ concentration. Lab Chip 19 (19), 3179–3189.
Yuce, M.R., 2010. Implementation of wireless body area networks for healthcare systems. Sensor Actuator Phys. 162 (1), 116–129.
Zephyr, 2020.
Zhang, H., Gutruf, P., Meacham, K., Montana, M.C., Zhao, X., Chiarelli, A.M., Vázquez-Guardado, A., Norris, A., Lu, L., Guo, Q., Xu, C., Wu, Y., Zhao, H., Ning, X., Bai, W., Kandela, I., Haney, C.R., Chanda, D., Gereau, R.W., Rogers, J.A., 2019a. Wireless, battery-free optoelectronic systems as subdermal implants for local tissue oximetry. Sci. Adv. 5 (3), eaaw0873.
Zhang, Y., Guo, H.X., Kim, S.B., Wu, Y.X., Ostojich, D., Park, S.H., Wang, X.J., Weng, Z. Y., Li, R., Bandodkar, A.J., Sekine, Y., Choi, J., Xu, S., Quaggin, S., Ghaffari, R., Rogers, J.A., 2019b. Passive sweat collection and colorimetric analysis of biomarkers relevant to kidney disorders using a soft microfluidic system. Lab Chip 19 (9), 1545–1555.
Zhang, Y.H., Webb, R.C., Luo, H.Y., Xue, Y.G., Kurniawan, J., Cho, N.H., Krishnan, S., Li, Y.H., Huang, Y.G., Rogers, J.A., 2016. Theoretical and experimental studies of epidermal heat flux sensors for measurements of core body temperature. Adv. Healthc. Mater. 5 (1), 119–127.
Zhao, F.J., Bonmarin, M., Chen, Z.C., Larson, M., Fay, D., Runnoe, D., Heikenfeld, J., 2020a. Ultra-simple wearable local sweat volume monitoring patch based on swellable hydrogels. Lab Chip 20 (1), 168–174.
Zhao, J.Q., Lin, Y.J., Wu, J.B., Nyein, H.Y.Y., Bariya, M., Tai, L.C., Chao, M.H., Ji, W.B., Zhang, G., Fan, Z.Y., Javey, A., 2019. A fully integrated and self-powered smartwatch for continuous sweat glucose monitoring. ACS Sens. 4 (7), 1925–1933.
Zhao, Y.C., Wang, B., Hojaiji, H., Wang, Z.Q., Lin, S.Y., Yeung, C., Lin, H.S., Nguyen, P., Chiu, K.L., Salahi, K., Cheng, X.B., Tan, J.W., Cerrillos, B.A., Emaminejad, S., 2020b. A wearable freestanding electrochemical sensing system. Sci. Adv. 6 (12).
Zhu, H.C., Cao, R.L., 2012. The relationship between serum levels of uric acid and prognosis of infection in critically ill patients. World J. Emerg. Med. 3 (3), 186–190.